Journal of The Electrochemical Society

OPEN ACCESS

A Discussion of the Cell Voltage during Discharge of an Intercalation Electrode for Various C-Rates Based on Non-Equilibrium Thermodynamics and Numerical Simulations

To cite this article: Manuel Landstorfer 2020 *J. Electrochem. Soc.* **167** 013518

Journal of The Electrochemical Society, 2020 **167** 013518

A Discussion of the Cell Voltage during Discharge of an Intercalation Electrode for Various C-Rates Based on Non-Equilibrium Thermodynamics and Numerical Simulations

Manuel Landstorfer [z]

Weierstrass Institute for Applied Analysis and Stochastics (WIAS) 10117 Berlin, Germany

In this work we discuss the modeling procedure and validation of a non-porous intercalation half-cell during galvanostatic discharge. The modeling is based on continuum thermodynamics with non-equilibrium processes in the active intercalation particle, the electrolyte, and the common interface where the intercalation reaction $Li^+ + e^- \rightleftharpoons Li$ occurs. The model is in detail investigated and discussed in terms of scalings of the non-equilibrium parameters, i.e. the diffusion coefficients D_A and D_E of the active phase and the electrolyte, conductivity σ_A and σ_E of both phases, and the exchange current density $e_0 L$, with numerical solutions of the underlying PDE system. The current density i as well as all non-equilibrium parameters are scaled with respect to the 1-C current density i_A^C of the intercalation electrode. We compute then numerically the cell voltage E as function of the capacity Q and the C-rate C_h. Within a hierarchy of approximations we provide computations of $E(Q)$ for various scalings of the diffusion coefficients, the conductivities and the exchange current density. For the later we provide finally a discussion for possible concentration dependencies.
 [DOI: 10.1149/2.0182001JES]

Manuscript submitted July 17, 2019; revised manuscript received October 17, 2019. Published November 19, 2019. *This paper is part of the JES Focus Issue on Mathematical Modeling of Electrochemical Systems at Multiple Scales in Honor of Richard Alkire.*

Lithium ion batteries (LIBs) are vital today for many branches of modern society and especially for electro-mobility. The german national platform electro-mobility aims one million electric vehicles by 2020, as well as the U.S., while China targets about five million zero emission cars. To achieve these goals, substantial knowledge on the effectively non-linear behavior of LiBs is required in order to reduce cost, increase their efficiency, safety, durability and further. The interpretation of experimental data requires a versatile and predictive mathematical model of a LIB, which accounts for the many physicochemical processes occurring simultaneously during charge and discharge, e.g. Li^+ diffusion in the electrolyte, surface reactions at the electrode/electrolyte interface, solid state diffusion in the active particles, and electrical conductivity.

First academic steps to model the functional principle of LIBs with the purpose of simulating their charge/discharge behavior were carried out by Newman et al. around 1993.[1] This electrochemical model became a central tool to interpret measured data of intercalation batteries. One of the central ingredients of the Newman model is the Butler–Volmer-type reaction rate R for the intercalation reaction $Li^+ + e^- \rightleftharpoons Li$ occurring at the interface $\Sigma_{A,E}$ between an intercalation electrode (particle) Ω_A and the electrolyte Ω_E. The actual functional dependency of $R = R(n_E, \varphi_E, n_A, \varphi_A)$ on the different variables of the equation system, e.g. the electrolyte concentration n_E, the electrostatic potential φ_E in the electrolyte, the concentration n_A of intercalated ions, and the electrostatic potential φ_A of the active phase, is, however, rather stated then derived. Especially the so called exchange current density and its functional relationship to the cation concentration is doubtable.

From a non-equilibrium thermodynamics (NET) point of view, the functional dependency $R = R(n_E, \varphi_E, n_A, \varphi_A)$ can be consistently derived and NET restricts this functional dependency in a very specific manner. We discuss in this work the modeling procedure of a single transfer reaction at the interface between an active intercalation phase and some electrolyte based on the framework of NET for volumes and surfaces and draw some conclusions regarding thermodynamic consistent models of the reaction rate. We account also for diffusion processes in the adjacent active particle and the electrolyte, as well es electrical conductivity, and state the corresponding balance equations. Then we consider galvanostatic discharge in half cell of some cathode intercalation material, electrolyte, and a lithium reference electrode, which is considered as ideally polarizable counter electrode.

We introduce the C_1-current density, i.e. the current at which the electrode is completely discharged during one hour, and scale all non-equilibrium parameters based on the C-rate C_h, i.e. multiples of the C_1 current density. It is then possible to derive a general relation between the measured cell voltage E, the capacity Q, and the C-rate C_h based on the reaction rate $R = R(n_E, \varphi_E, n_A, \varphi_A)$. Since, however, actually the concentrations at the interface $\Sigma_{A,E}$ of intercalated cations n_A and electrolytic cations n_E enter the surface reaction rate R, we need to solve necessarily the diffusion equations in the adjacent phases. We discuss various approximation regimes and parameter scalings of the non-equilibrium parameters which allows us to compare numerical simulations of cell voltage $E = E(Q, C_h)$ to some representative experimental examples, especially of $Li_x(Ni_{1/3}Mn_{1/3}Co_{1/3}O_2$(NMC). Fig. 1 shows the measured cell voltage E as function of the capacity (or status of charge) for various discharge rates of thin of NMC half cell.[2]

We show that a rather *simple* (but thermodynamically consistent) model of the surface reaction rate R, or more precise of the exchange current density, is sufficient to understand and predict the complex non-linear behavior of the cell voltage as function of the capacity Q and the C-Rate C_h. We provide also computations of $E = E(Q, C_h)$ for the exchange current density introduced by *Newman* et al., draw

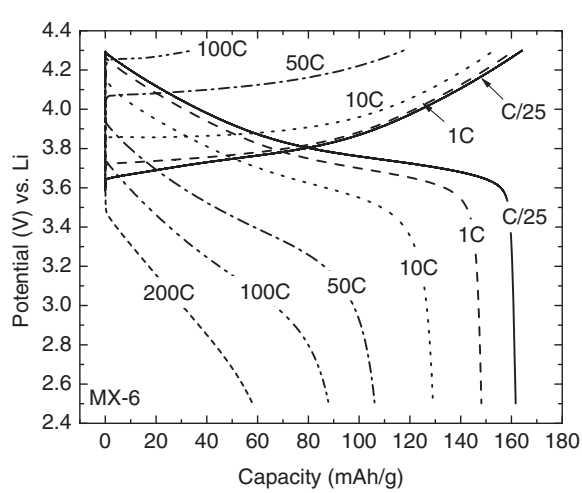

Figure 1. Discharge curves (lower part) for various C-rates (Data of Fig 1b from Ref. 2, reprinted with permission of The Electrochemical Society).

[z]E-mail: Manuel.Landstorfer@wias-berlin.de

some conclusions regarding thermodynamic consistency, and compare computations based on this expression to the cell voltage based on our *simple* expression of the current density.

Modeling

We consider an active intercalation particle Ω_{A} in contact with some electrolyte Ω_{E}. The interface $\Sigma_{\mathrm{A,E}} = \Omega_{\mathrm{A}} \cap \Omega_{\mathrm{E}}$ captures the actual surface Σ_{A} of the active particle as well as the electrochemical double layer forming at the interface, i.e. $\Sigma_{\mathrm{A,E}} = \Omega_{\mathrm{A}}^{\mathrm{SCL}} \cup \Sigma_{\mathrm{A}} \cup \Omega_{\mathrm{E}}^{\mathrm{SCL}}$. The domains Ω_{E} and Ω_{A} are thus electro-neutral, and we refer to Refs. 3–5 for details on the derivation. The electrolyte is on the right side in contact to some metallic counter electrode Ω_{R}, where the interface $\Sigma_{\mathrm{E,C}}$ captures also the double layer forming at the interface between the electrolyte and the counter electrode Ω_{C}.

We consider a 1D approximation, where the electrode-electrolyte interface $\Sigma_{\mathrm{A,E}}$ is positioned at $x = x_{\mathrm{AE}}$, the left boundary of Ω_{A} is denoted by $x = 0$ and the right boundary of Ω_{E} is $x = x_{\mathrm{EC}}$, with $d_{\mathrm{A}} = |x_{\mathrm{AE}}|$ and $d_{\mathrm{E}} = |x_{\mathrm{EC}} - x_{\mathrm{AE}}|$. The counter electrode is positioned at $x = x_{\mathrm{EC}}$ and spans to $x = x_{\mathrm{C}}$.

For some quantity $u(x, t)$, we denote with

$$u|_{\mathrm{AE}}^{\pm} = u|_{x=x_{\mathrm{AE}}}^{\mp} \quad \text{and} \quad u|_{\mathrm{EC}}^{\pm} = u|_{x=x_{\mathrm{EC}}}^{\mp} \tag{1}$$

the evaluation at the respective side of the interface $\Sigma_{\mathrm{A,E}}$ and $\Sigma_{\mathrm{E,C}}$. If u is present only on one phase, we drop the superscript $^{\pm}$.

The active particle Ω_{A} is a mixture of electrons e^-, intercalated cations C and lattice ions M^+, and the electrolyte a mixture of solvated cations C^+, solvated anions A^- and solvent molecules S. The respective species densities are denoted with $n_\alpha(\mathbf{x}, t), \mathbf{x} \in \Omega_i$. We denote with

$$\mu_\alpha := \frac{\partial \psi}{\partial n_\alpha}, \qquad \alpha = \mathrm{E}_A, \mathrm{E}_C, \mathrm{E}_S, \mathrm{A}_C, \mathrm{A}_e, \mathrm{A}_M, \tag{2}$$

the chemical potential of the constituents, which are derived from a free energy density[6,7] $\psi = \psi_{\mathrm{A}} + \psi_{\mathrm{E}}$ with $\psi_{\mathrm{A}} = \hat{\psi}_{\mathrm{A}}(n_{\mathrm{A}_e}, n_{\mathrm{A}_C}, n_{\mathrm{A}_M})$ of the active particle and $\psi_{\mathrm{E}} = \hat{\psi}(n_{\mathrm{E}_S}, n_{\mathrm{E}_A}, n_{\mathrm{E}_C})$ of the electrolyte phase.

For the surface Σ we have surface chemical potentials[4,6,8,9]

$$\underset{s}{\mu}_\alpha := \frac{\partial \underset{s}{\psi}}{\partial \underset{s}{n}_\alpha}, \quad \alpha = \mathrm{E}_A, \mathrm{E}_C, \mathrm{E}_S, \mathrm{A}_C, \mathrm{A}_e, \mathrm{A}_M, \tag{3}$$

which are derived from some general surface free energy density $\underset{s}{\psi}$.

Material functions.—For the electrolyte we consider exclusively the material model[9–11] of an incompressible liquid electrolyte accounting for solvation effects, i.e.

$$\mu_\alpha = g_\alpha^R + k_{\mathrm{B}} T \ln(y_\alpha) + v_\alpha^R (p - p^R), \quad \alpha = \mathrm{E}_S, \mathrm{E}_A, \mathrm{E}_C, \tag{4}$$

with mole fraction

$$y_\alpha = \frac{n_\alpha}{n_{\mathrm{E}}^{\mathrm{tot}}}, \tag{5}$$

molar concentration n_α, and total molar concentration of the mixture (with respect to the number of mixing particles[9])

$$n_{\mathrm{E}}^{\mathrm{tot}} = n_{\mathrm{E}_S} + n_{\mathrm{E}_A} + n_{\mathrm{E}_C}. \tag{6}$$

In (4) T denotes temperature, k_{B} the Boltzmann constant, g_α^R denotes the reference molar Gibbs free energy (or chemical potential of the pure substance), p^R the reference pressure and v_α^R the partial molar volume of constituent α in the mixture. Throughout this manuscript we assume an isothermal temperature of $T = 298.15$ [K].

Note that n_{E_S} denotes the number of *free* solvent molecules, whereas n_{E_A} and n_{E_C} are the densities of the solvated ions. This is crucial for various aspects of the thermodynamic model, and we refer to Refs. 9,10,12,13 for details. Overall, the material model for the electrolyte corresponds to an incompressible mixture with solvation effects. We assume further

$$\frac{v_{\mathrm{E}_C}^R}{v_{\mathrm{E}_S}^R} = \frac{m_{\mathrm{E}_C}}{m_{\mathrm{E}_S}} \quad \text{and} \quad \frac{v_{\mathrm{E}_A}^R}{v_{\mathrm{E}_S}^R} = \frac{m_{\mathrm{E}_A}}{m_{\mathrm{E}_S}} \tag{7}$$

whereby the incompressibility constraint[9–11] implies also a conservation of mass, i.e.

$$\sum_\alpha v_\alpha^R n_\alpha = 1 \quad \Leftrightarrow \quad \sum_\alpha m_\alpha n_\alpha = \rho = \frac{m_{\mathrm{E}_S}}{v_{\mathrm{E}_S}^R} = \text{const.}. \tag{8}$$

The molar volume of the solvent is related to the mole density $n_{\mathrm{E}_S}^R$ of the pure solvent as

$$v_{\mathrm{E}_S}^R = (n_{\mathrm{E}_S}^R)^{-1}. \tag{9}$$

Note further that the partial molar volumes v_α^R and the molar masses m_α of the cation and anion are related to the solvation number κ_{E_C} and κ_{A_C}, respectively.

We assume that the partial molar volume of the ionic species is mainly determined by the solvation shell, which seems reasonable for large solvents like DMC in comparison to the small ions like Li^+. We proceed thus with the assumption

$$v_{\mathrm{E}_C} = \kappa_{\mathrm{E}} \cdot v_{\mathrm{E}_S} \quad \text{and} \quad v_{\mathrm{E}_A} = \kappa_{\mathrm{E}} \cdot v_{\mathrm{A}_C}. \tag{10}$$

For the active particle, we consider an extension of a classical lattice mixture model[14–21] which accounts for occupation numbers $\omega_{\mathrm{A}} > 1$ as well as a Redlich–Kister type enthalpy term[22,23] for the intercalation material $\mathrm{Li}_y(\mathrm{Ni}_{1/3}\mathrm{Mn}_{1/3}\mathrm{Co}_{1/3})\mathrm{O}_2$ (NMC). We refer to Ref. 24 for a detailed discussion and derivation based on a free energy ψ^{A}. The chemical potential of intercalated lithium is derived as

$$\mu_{\mathrm{A}_C} = k_{\mathrm{B}} T \left(\ln\left(\frac{\frac{1}{\omega_{\mathrm{A}}} y_{\mathrm{A}_C}}{1 + \frac{1-\omega_{\mathrm{A}}}{\omega_{\mathrm{A}}} y_{\mathrm{A}_C}} \right) - \omega_{\mathrm{A}} \cdot \ln\left(\frac{1 - y_{\mathrm{A}_C}}{1 + \frac{1-\omega_{\mathrm{A}}}{\omega_{\mathrm{A}}} y_{\mathrm{A}_C}} \right) + \gamma_{\mathrm{A}} \cdot h_{\mathrm{A}}(y_{\mathrm{A}_C}) \right) \tag{11}$$

with

$$h_{\mathrm{A}}(y) := (2y-1) + \frac{1}{2}\big(6y(1-y) - 1\big) - \frac{1}{3}\big(8y(1-y) - 1\big)(2y-1) \tag{12}$$

and mole fraction

$$y_{\mathrm{A}_C} = \frac{n_{\mathrm{A}_C}}{n_{\mathrm{A}_\ell}} =: y_{\mathrm{A}} \tag{13}$$

of intercalated cations in the active phase. The number density n_{A_ℓ} of lattice sites is constant, which corresponds to an incompressible lattice, and the enthalpy parameter $\gamma_{\mathrm{A}} < 2.5$. Note that $\gamma_{\mathrm{A}} > 2.5$ entails a phase separation[20] and requires an additional term $\gamma_{\mathrm{A}} \mathrm{div} \nabla y_{\mathrm{A}_C}$ in the chemical potential. However, we assume throughout this work that no phase separation occurs, whereby in diffusional equilibrium of the intercalation phase the concentration is homogeneous. An extension of this discussion toward phase separating materials will given in a subsequent work.

For the electrons we consider[9,25]

$$\mu_{\mathrm{A}_e} = \left(\frac{3}{8\pi}\right)^{\frac{2}{3}} \frac{h^2}{2m_{\mathrm{A}_e}} n_{\mathrm{A}_e}^{\frac{2}{3}} \quad \text{and} \quad \underset{s}{\mu}_{\mathrm{A}_e} = \underset{s}{g}_{\mathrm{A}_e}^R = \text{const.} \tag{14}$$

and for the lattice ions

$$\mu_{\mathrm{A}_M} = g_{\mathrm{A}_M}^R + k_{\mathrm{B}} T \ln\left(1 - y_{\mathrm{A}_C}\right) + v_{\mathrm{M}}^R (p_{\mathrm{M}} - p_{\mathrm{M}}^R), \tag{15}$$

where $v_{\mathrm{M}}^R = (n_{\mathrm{M}}^R)^{-1}$ is the molar volume of the lattice ions, p_{M} the partial pressure and $g_{\mathrm{A}_M}^R$ the constant molar Gibbs energy. The material functions of the active intercalation electrode is essentially model an incompressible solid with a sub-lattice for the intercalated cations A_C.

The explicit surface chemical potentials

$$\underset{s}{\mu}_\alpha = \frac{\partial \underset{s}{\psi}}{\partial \underset{s}{n}_\alpha}, \qquad \alpha = \mathrm{E}_A, \mathrm{E}_C, \mathrm{E}_S, \mathrm{A}_C, \mathrm{A}_M, \tag{16}$$

are not required throughout this work since we will assume that the double layer is in equilibrium and that the double layer capacity (and thus also adsorption), is negligible for the sake of this work. However, we refer to Ref. 9 for the explicit functions of $\underset{s}{\mu_\alpha}$ and the surface free energy of a surface lattice mixture with solvation effects.

Electroneutrality condition.—The electroneutrality condition of Ω_{A}, Ω_{E} and Ω_{C} can be obtained by an asymptotic expansion of the balance equations in the electrochemical double layer at the respective surface Σ. We only briefly recapture the central conclusions and refer to Refs. 3–5,9,26 for details on the modeling, validation and the asymptotics. Most importantly, we have that

- the double layer is in thermodynamic equilibrium, i.e. $\nabla\mu_\alpha + e_0 z_\alpha \nabla\varphi = 0$ in $\Omega_{\mathrm{A}}^{\mathrm{SCL}}$ and $\Omega_{\mathrm{E}}^{\mathrm{SCL}}$, where e_0 is the elementary charge, z_α the charge number and φ the electrostatic potential
- there exists a potential drop between the active particle surface Σ and the hyper-surface $\Sigma_{\mathrm{A,E}}^{\pm}$ outside of the respective space charge layers which is denoted by

$$U_i^{\mathrm{SCL}} := \underset{s}{\varphi} - \varphi|_{\mathrm{AE}}^{\pm} \qquad [17]$$

where $\varphi|_{\mathrm{AE}}^{\pm}$ is the electrostatic potential *right outside* the space charge layer in the electrolyte or the active particle, respectively, and $\underset{s}{\varphi}$ the (continuous) potential at the surface Σ[a]. The whole potential drop across the double layer at $\Sigma_{\mathrm{A,E}}$ is denoted by

$$U_{\mathrm{AE}}^{\mathrm{DL}} := U_{\mathrm{E}}^{\mathrm{SCL}} - U_{\mathrm{A}}^{\mathrm{SCL}} = \varphi|_{\mathrm{AE}}^{+} - \varphi|_{\mathrm{AE}}^{-} \qquad [18]$$

- the chemical potential at the surface can be *pulled back* through the double layer, i.e. $\underset{s}{\mu_\alpha} = \mu_\alpha^i - e_0 z_\alpha U_i^{\mathrm{SCL}}$, $i = \mathrm{A}, \mathrm{E}$
- the condition $\underset{s}{\mu_e} = \text{const.}$ entails that the potential drop $U_{\mathrm{A}}^{\mathrm{SCL}}$ is constant (with respect to some applied voltage) and determined by

$$U_{\mathrm{A}}^{\mathrm{SCL}} = \frac{1}{e_0}(\underset{s}{\mu_{\mathrm{A}_e}} - \mu_{\mathrm{A}_e}\big|_{\mathrm{AE}}). \qquad [19]$$

- the charge density in the electrolyte vanishes and that for monovalent electrolytes the cation mole fraction (or number density) is equal to the anion mole fraction, i.e.

$$y_{\mathrm{E}_C} = y_{\mathrm{A}_C} =: y_{\mathrm{E}}. \qquad [20]$$

- in the active phase the electroneutrality entails

$$n_{\mathrm{A}_e} = n_{\mathrm{A}_M} = \text{const.} \qquad [21]$$

whereby we abbreviate

$$g_{\mathrm{A}_e}^R := \mu_{\mathrm{A}_e}(n_{\mathrm{A}_M}) \qquad [22]$$

which is basically the Fermi energy of the solid material.

Transport equations.—In the electrolyte Ω_{E} we have two balance equations determining the concentration $n_{\mathrm{E}_C}(x,t)$ (or the mole fraction $y_{\mathrm{E}_C}(x,t)$) and the electrostatic potential $\varphi_{\mathrm{E}}(x,t)$ in the electrolyte,[27–32] i.e.

$$\frac{\partial n_{\mathrm{E}_C}}{\partial t} = -\partial_x J_{\mathrm{E}_C} \quad \text{with} \quad J_{\mathrm{E}_C} = -D_{\mathrm{E}} \cdot n_{\mathrm{E}}^{\mathrm{tot}}\, \Gamma_{\mathrm{E}}^{\mathrm{tf}} \cdot \partial_x y_{\mathrm{E}_C} + \frac{t_{\mathrm{E}_C}}{e_0} J_{\mathrm{E},q} \qquad [23]$$

$$0 = -\partial_x J_{\mathrm{E},q} \quad \text{with} \quad J_{\mathrm{E},q} = -S_{\mathrm{E}} \cdot n_{\mathrm{E}}^{\mathrm{tot}}\, \Gamma^{\mathrm{tf}} \partial_x y_{\mathrm{E}} - \Lambda_{\mathrm{E}} n_{\mathrm{E}} \partial_x \varphi_{\mathrm{E}} \qquad [24]$$

with (dimensionless) thermodynamic factor

$$\Gamma_{\mathrm{E}}^{\mathrm{tf}} := \frac{y_{\mathrm{E}_C}}{k_{\mathrm{B}}T}\frac{\partial \hat{\mu}_{\mathrm{E}_C}}{\partial y_{\mathrm{E}_C}} = 1 + 2\kappa_{\mathrm{E}}\frac{y_{\mathrm{E}}}{1 - 2y_{\mathrm{E}_C}} = \Gamma_{\mathrm{E}}^{\mathrm{tf}}(y_{\mathrm{E}}). \qquad [25]$$

where

$$\hat{\mu}_{\mathrm{E}_C} := \mu_{\mathrm{E}_C} - \frac{m_{\mathrm{E}_C}}{m_{\mathrm{E}_S}}\mu_{\mathrm{E}_S} = k_{\mathrm{B}}T\left(\ln\left(y_{\mathrm{E}_C}\right) - \kappa_{\mathrm{E}}\ln\left(y_{\mathrm{E}_S}\right)\right) \qquad [26]$$

is the thermodynamic driving force for diffusion,[11] and D_{E} the chemical diffusion coefficient, t_{E_C} the cation transfer number, and Λ_{E} the molar conductivity.

Note that we assumed $\frac{v_{\mathrm{E}_C}^R}{v_{\mathrm{E}_S}^R} = \frac{m_{\mathrm{E}_C}}{m_{\mathrm{E}_S}}$ and $v_{\mathrm{E}_C}^R = \kappa_{\mathrm{E}} \cdot v_{\mathrm{E}_S}^R$ which yields the representation 26. Note further that the total number density $n_{\mathrm{E}}^{\mathrm{tot}} = n_{\mathrm{E}_S} + n_{\mathrm{E}_C} + n_{\mathrm{E}_A}$ in the electrolyte writes as

$$n_{\mathrm{E}}^{\mathrm{tot}} = n_{\mathrm{E}_S}^R \cdot \frac{1}{1 + 2(\kappa_{\mathrm{E}} - 1)y_{\mathrm{E}}} = n_{\mathrm{E}}^{\mathrm{tot}}(y_{\mathrm{E}}) \qquad [27]$$

which is determined from the incompressibility constraint 8

$$v_{\mathrm{E}_S}^R n_{\mathrm{E}_S} + v_{\mathrm{E}_A}^R n_{\mathrm{E}_A} + v_{\mathrm{E}_C}^R n_{\mathrm{E}_C}^R = 1 \qquad [28]$$

and the electrolyte concentration n_{E_C} in terms of y_{E} as

$$n_{\mathrm{E}_C} = y_{\mathrm{E}_C} \cdot n = n_{\mathrm{E}_S}^R \frac{y_{\mathrm{E}_C}}{1 + 2(\kappa_{\mathrm{E}} - 1)y_{\mathrm{E}}} = n_{\mathrm{E}_C}(y_{\mathrm{E}}). \qquad [29]$$

If we consider a simple Nernst–Planck-flux relation for the cation and anion fluxes,[11,33] respectively, i.e.

$$\mathbf{J}_\alpha = D_\alpha^{\mathrm{NP}} \frac{n_\alpha}{k_{\mathrm{B}}T}\left(\nabla\mu_\alpha - \frac{m_\alpha}{m_0}\nabla\mu_{\mathrm{E}_S} + e_0 z_\alpha n_\alpha \nabla\varphi_{\mathrm{E}}\right) \qquad \alpha = \mathrm{E}_A, \mathrm{E}_C, \qquad [30]$$

with constant diffusion coefficients $D_{\mathrm{E}_A}^{\mathrm{NP}}$ for the anion and $D_{\mathrm{E}_C}^{\mathrm{NP}}$ for the cation, we obtain (in the electroneutral electrolyte)

$$D_{\mathrm{E}} = \frac{2D_{\mathrm{E}_C}^{\mathrm{NP}} \cdot D_{\mathrm{E}_A}^{\mathrm{NP}}}{D_{\mathrm{E}_A}^{\mathrm{NP}} + D_{\mathrm{E}_C}^{\mathrm{NP}}} \quad t_{\mathrm{E}_C} = \frac{D_{\mathrm{E}_C}^{\mathrm{NP}}}{D_{\mathrm{E}_A}^{\mathrm{NP}} + D_{\mathrm{E}_C}^{\mathrm{NP}}} \qquad [31]$$

$$\Lambda_{\mathrm{E}} = \frac{e_0^2}{k_{\mathrm{B}}T}(D_{\mathrm{E}_A}^{\mathrm{NP}} + D_{\mathrm{E}_C}^{\mathrm{NP}}) \quad S_{\mathrm{E}} = e_0(D_{\mathrm{E}_C}^{\mathrm{NP}} - D_{\mathrm{E}_A}^{\mathrm{NP}}) \qquad [32]$$

Note, however, for general Maxwell-Stefan type diffusion[29–32,34] or cross-diffusion coefficients[7,24,35] in the cation and anion fluxes lead to more *complex* representations of the transport parameters $(t_{\mathrm{E}_C}, S_{\mathrm{E}}, D_{\mathrm{E}}, \Lambda_{\mathrm{E}})$. In general, three of the transport parameters are *independent*, and S_{E}, t_{E_C} and Λ_{E} are related to each other via

$$\frac{k_{\mathrm{B}}T}{e_0}(2t_C - 1) = \frac{S_{\mathrm{E}}}{\Lambda_{\mathrm{E}}}. \qquad [33]$$

Further, $(t_{\mathrm{E}_C}, S_{\mathrm{E}}, D_{\mathrm{E}}, \Lambda_{\mathrm{E}})$ depend in general non-linearly on the electrolyte concentration n_{E_C}. However, it is sufficient for the sake of this work to assume constant values for the transport parameters $(t_{\mathrm{E}_C}, S_{\mathrm{E}}, D_{\mathrm{E}}, \Lambda_{\mathrm{E}})$, together with relation 33.

In the active particle Ω_{A} we have two balance equations determining the concentration $n_{\mathrm{A}_C}(x,t)$ (or mole fraction y_{A_C}) and the electrostatic potential $\varphi_{\mathrm{A}}(x,t)$ in the active particle, i.e.

$$\frac{\partial n_{\mathrm{A}_C}}{\partial t} = -\partial_x J_{\mathrm{A}_C} \quad \text{with} \quad J_{\mathrm{A}_C} = -D_{\mathrm{A}} \cdot n_{\mathrm{A}_\ell}\, \Gamma_{\mathrm{A}}^{\mathrm{tf}} \cdot \partial_x y_{\mathrm{A}_C} \qquad [34]$$

$$0 = -\partial_x J_{\mathrm{A},q} \quad \text{with} \quad J_{\mathrm{A},q} = -\sigma_{\mathrm{A}} \partial_x \varphi_{\mathrm{A}} \qquad [35]$$

and (dimensionless) thermodynamic factor

$$\Gamma_{\mathrm{A}}^{\mathrm{tf}} = \frac{y_{\mathrm{A}}}{k_{\mathrm{B}}T}\frac{\partial\mu_{\mathrm{A}}}{\partial y_{\mathrm{A}}} = 1 + \frac{y_{\mathrm{A}}}{1 - y_{\mathrm{A}}} - 2\gamma_{\mathrm{A}} y_{\mathrm{A}} = \Gamma_{\mathrm{A}}^{\mathrm{tf}}(y_{\mathrm{A}}). \qquad [36]$$

Note that in principle σ_{A} can be dependent on the amount of intercalated ions, i.e. $\sigma_{\mathrm{A}} = \sigma_{\mathrm{A}}(y_{\mathrm{A}})$.

Reaction rate based on surface thermodynamics.—We want to investigate the non-equilibrium thermodynamic modeling of the intercalation reaction

$$\mathrm{Li}^+\big|_{\mathrm{E}} + \mathrm{e}^-\big|_{\mathrm{A}} \rightleftharpoons \mathrm{Li}\big|_{\mathrm{A}} + \kappa_{\mathrm{E}} \cdot \mathrm{S}\big|_{\mathrm{E}}. \qquad [37]$$

Surface thermodynamics dictates that the reaction rate $\underset{s}{R}$ of this process can in general be written as[4,5,13,36,37]

$$\underset{s}{R} = \underset{s}{L} \cdot \left(\mathrm{e}^{\alpha \cdot \frac{1}{k_{\mathrm{B}}T}\underset{s}{\lambda}} - \mathrm{e}^{-(1-\alpha)\cdot\frac{1}{k_{\mathrm{B}}T}\underset{s}{\lambda}}\right) \quad \text{with}$$

$$\underset{s}{\lambda} = \underset{s}{\mu_{\mathrm{A}_C}} + \kappa_{\mathrm{E}} \cdot \underset{s}{\mu_{\mathrm{E}_S}} - \underset{s}{\mu_{\mathrm{E}_C}} - \underset{s}{\mu_{\mathrm{A}_e}}, \qquad [38]$$

[a]Note that the continuity of φ across Σ is an assumption.

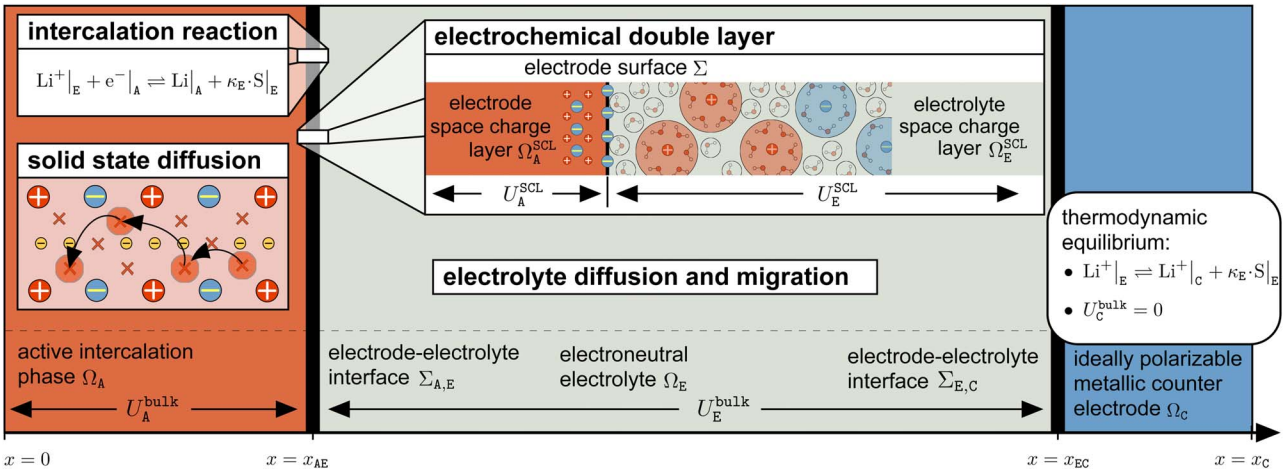

Figure 2. Sketch of an active intercalation phase Ω_{A} in contact with some electrolyte Ω_{E}. The electrode-electrolyte interface $\Sigma_{\mathrm{A,E}}$ covers the space charge layer $\Omega_{\mathrm{E}}^{\mathrm{SCL}}$ of the electrolyte and $\Omega_{\mathrm{A}}^{\mathrm{SCL}}$ of the electrode as well as the actual electrode surface Σ. Several processes occur simultaneously, i.e. the intercalation reaction, electrolyte diffusion and solid state diffusion as well es electrical conductivity.

with $\alpha \in [0, 1]$. Note that a non-negative function $\underset{s}{L}$ in 38 ensures a non-negative entropy production $\underset{s}{r}_{\sigma,R}$ due to reactions on the surface, i.e. $\underset{s}{r}_{\sigma,R} = \underset{s}{\lambda} \cdot \underset{s}{R} > 0$.

The quantity $\underset{s}{\lambda}$ can be considered as surface affinity of the Reaction 37. The surface reaction rate R vanishes when the affinity vanishes, which is the actually the thermodynamic equilibrium condition of 37, i.e. $\underset{s}{\lambda} = 0 \Leftrightarrow \underset{s}{r}_{\sigma,R} = 0$.

Since the electrochemical double layer is in equilibrium, we can *pull back* the surface chemical potentials $\underset{s}{\mu}_{\alpha}$ through the double layer to the respective *points* (in an asymptotic sense) outside of the double layer, whereby we obtain for the surface affinity

$$\underset{s}{\lambda} = \mu_{\mathrm{A}_C}\big|_{\mathrm{AE}}^{-} + \kappa_{\mathrm{E}} \cdot \mu_{\mathrm{E}_S}\big|_{\mathrm{AE}}^{+} - \mu_{\mathrm{E}_C}\big|_{\mathrm{AE}}^{+} + e_0 U_{\mathrm{A,E}}^{\mathrm{DL}} - \mu_{\mathrm{A}_e}\big|_{\mathrm{AE}}^{-}. \qquad [39]$$

With the material models 4 and 11 we can rewrite the surface affinity as

$$\underset{s}{\lambda} = e_0(U_{\mathrm{AE}}^{\mathrm{DL}} - E_{\mathrm{A,E}}^{T}) + k_{\mathrm{B}}T\left(f_{\mathrm{A}}(y_{\mathrm{A}_C}|_{\mathrm{AE}}) - f_{\mathrm{E}}(y_{\mathrm{E}_C}|_{\mathrm{AE}})\right) \qquad [40]$$

with

$$E_{\mathrm{A,E}}^{T} := \frac{1}{e_0}(g_{\mathrm{E}_C}^{R} + g_{\mathrm{A}_e}^{R} - g_{\mathrm{A}_C}^{R} - \kappa_{\mathrm{E}} g_{\mathrm{E}_S}^{R}) \qquad [41]$$

and

$$f_{\mathrm{E}}(y_{\mathrm{E}_C}) := \ln\left(\frac{y_{\mathrm{E}_C}}{\left(\hat{y}_{\mathrm{E}_S}(y_{\mathrm{E}_C})\right)^{\kappa_{\mathrm{E}}}}\right) \quad , \qquad [42]$$

$$f_{\mathrm{A}}(y_{\mathrm{A}_C}) := \ln\left(\frac{\frac{1}{\omega_{\mathrm{A}}} y_{\mathrm{A}_C}}{1 + \frac{1-\omega_{\mathrm{A}}}{\omega_{\mathrm{A}}} y_{\mathrm{A}_C}}\right) - \omega_{\mathrm{A}} \cdot \ln\left(\frac{1 - y_{\mathrm{A}_C}}{1 + \frac{1-\omega_{\mathrm{A}}}{\omega_{\mathrm{A}}} y_{\mathrm{A}_C}}\right) + \gamma_{\mathrm{A}} \cdot h_{\mathrm{A}}(y_{\mathrm{A}_C}) \qquad [43]$$

with h_{A} according to 12. Note again that $y_{\mathrm{A}_C}|_{\mathrm{AE}}$ denotes the evaluation of y_{A_C} at the interface $\Sigma_{\mathrm{A,E}}$ and that the surface affinity 40 is dependent on the chemical potential (or the mole fraction) evaluated at the interface.

Cell Voltage.—We consider the cell voltage in a half cell with metallic lithium as counter electrode, denoted by C and position at $x = x_{\mathrm{EC}}$ (see Fig. 2. The cell voltage in such a cell is

$$E = \underbrace{\varphi|_{x=0} - \varphi|_{\mathrm{AE}}^{+}}_{=:-U_{\mathrm{A}}^{\mathrm{bulk}}} + \underbrace{\varphi|_{\mathrm{AE}}^{+} - \varphi|_{\mathrm{AE}}^{-}}_{=U_{\mathrm{AE}}^{\mathrm{DL}}} + \underbrace{\varphi|_{\mathrm{AE}}^{+} - \varphi|_{\mathrm{EC}}^{-}}_{=:U_{\mathrm{E}}^{\mathrm{bulk}}} + \underbrace{\varphi|_{\mathrm{EC}}^{-} - \varphi|_{\mathrm{EC}}^{+}}_{U_{\mathrm{EC}}^{\mathrm{DL}}} + \underbrace{\varphi|_{x=x_{\mathrm{EC}}}^{+} - \varphi|_{x=x_{\mathrm{C}}}}_{=:U_{\mathrm{C}}^{\mathrm{bulk}}}, \qquad [44]$$

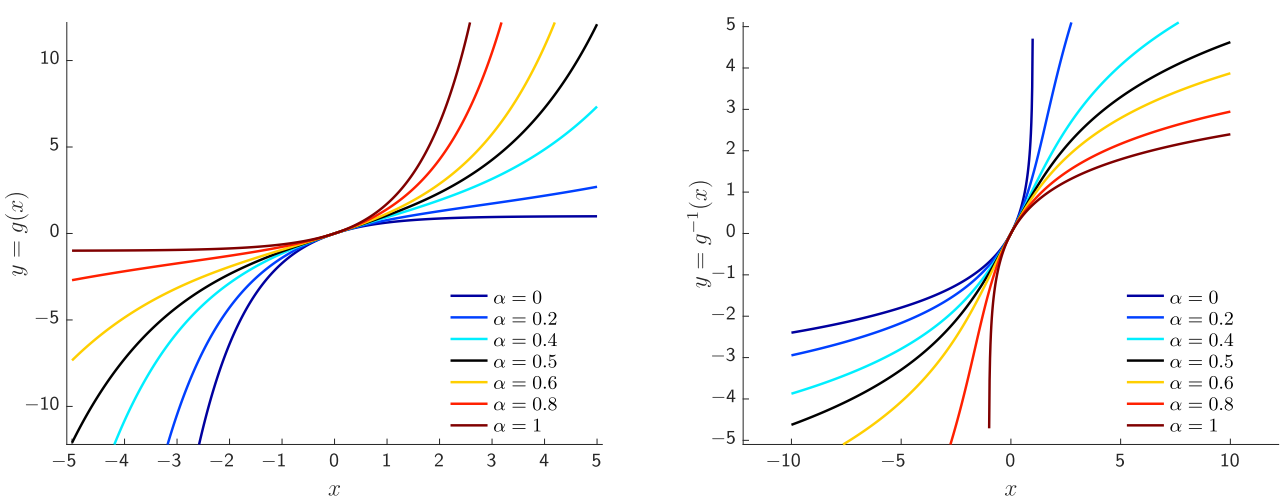

Figure 3. Reaction rate function $g(x) = \mathrm{e}^{\alpha \cdot x} - \mathrm{e}^{-(1-\alpha)\cdot x}$ and its inverse g^{-1} for various values of α.

where $U_{\mathrm{A}}^{\mathrm{bulk}}$ is the potential drop in the bulk active particle due to the electron transport, $U_{\mathrm{A,E}}^{\mathrm{DL}}$ is the potential drop across the double layer at the interface between the active particle and the electrolyte, and $U_{\mathrm{E}}^{\mathrm{bulk}}$ the bulk potential drop due to cation electric current.

We assume that the counter electrode Ω_{C} is *ideally polarizable*,[28] whereby the reaction

$$\mathrm{Li}^+\big|_{\mathrm{C}} + \kappa_{\mathrm{E}} \cdot \mathrm{S}\big|_{\mathrm{E}} \rightleftharpoons \mathrm{Li}^+\big|_{\mathrm{E}} \qquad [45]$$

at the the interface $\Sigma_{\mathrm{E,C}}$ positioned at $x = x_{\mathrm{EC}}$ is in thermodynamic equilibrium and $U_{\mathrm{C}}^{\mathrm{bulk}} = \varphi|_{x=x_{\mathrm{EC}}}^{-} - \varphi|_{x=x_{\mathrm{C}}} = 0$. The equilibrium condition of 45 entails

$$U_{\mathrm{EC}}^{\mathrm{DL}} = \varphi|_{x=x_{\mathrm{EC}}}^{-} - \varphi|_{x=x_{\mathrm{EC}}}^{+} = \frac{1}{e_0}\left(\mu_{\mathrm{C}_C} - \mu_{\mathrm{E}_C}\big|_{\mathrm{EC}}^{-} + \kappa_{\mathrm{E}}\mu_{\mathrm{E}_S}\big|_{\mathrm{EC}}^{-}\right) \qquad [46]$$

$$= \frac{1}{e_0}(\mu_{\mathrm{C}_C} - g_{\mathrm{A}_C}^R - \kappa_{\mathrm{E}} g_{\mathrm{E}_S}^R) - \frac{k_{\mathrm{B}}T}{e_0} f_{\mathrm{E}}(y_{\mathrm{E}_C}\big|_{\mathrm{EC}}) \qquad [47]$$

where $\mu_{\mathrm{C}_C} = \text{const.}$ is the chemical potential of the metallic lithium.

For the surface affinity 40 we obtain the compact typeface

$$\underset{s}{\lambda} = e_0(E + U_{\mathrm{A}}^{\mathrm{bulk}} - U_{\mathrm{E}}^{\mathrm{bulk}} - E_{\mathrm{A,C}}) + k_{\mathrm{B}}T\left(f_{\mathrm{A}} - f_{\mathrm{E}}|_{\mathrm{AE}} + f_{\mathrm{E}}|_{\mathrm{EC}}\right) \qquad [48]$$

with

$$E_{\mathrm{A,C}} = \frac{1}{e_0}(\mu_{\mathrm{C}_C} - g_{\mathrm{A}_C}^R + g_{\mathrm{A}_e}^R). \qquad [49]$$

and

$$f_{\mathrm{E}}|_{\mathrm{AE}} = f_{\mathrm{E}}(y_{\mathrm{E}_C}|_{\mathrm{AE}}) \quad \text{and} \quad f_{\mathrm{E}}|_{\mathrm{EC}} = f_{\mathrm{E}}(y_{\mathrm{E}_C}|_{\mathrm{EC}}). \qquad [50]$$

Current–Voltage relation.—For the single intercalation reaction we have the following expression[4]

$$i = -e_0 \underset{s}{R} + C_{\mathrm{E}}^{\mathrm{DL}} \cdot \frac{dU_{\mathrm{E}}^{\mathrm{SCL}}}{dt} \qquad [51]$$

for the current density i flowing out of the electrode Ω_{A}, where $C_{\mathrm{E}}^{\mathrm{DL}}$ is the double layer capacity. Note that the reaction rate is

$$\underset{s}{R} = \underset{s}{L} \cdot g\left(\frac{1}{k_{\mathrm{B}}T}\underset{s}{\lambda}\right) \quad \text{with} \quad g(x) = \left(\mathrm{e}^{\alpha \cdot x} - \mathrm{e}^{-(1-\alpha)\cdot x}\right). \qquad [52]$$

Since $g(x)$ is a strictly monotone function, we can introduce the inverse of g, i.e. g^{-1}. For $\alpha = \frac{1}{2}$ we have $g(x) = 2\sinh\left(\frac{1}{2}x\right)$ and $g^{-1}(y) = 2g^{-1}\left(\frac{1}{2}x\right)$. For values $\alpha \neq 0.5$ the inverse function g^{-1} is only implicitly given, however, can easily be calculated numerically. Fig. 3 display the functions g and g^{-1} for various values of α. We call $g(x)$ the reaction rate function and g^{-1} the inverse reaction rate function.

Note that in the Tafel approximation $g(\frac{1}{k_{\mathrm{B}}T}\underset{s}{\lambda}) \approx \frac{1}{k_{\mathrm{B}}T}\underset{s}{\lambda}$ Eq. 51 yields[b]

$$\frac{e_0}{k_{\mathrm{B}}T}U_{\mathrm{E}}^{\mathrm{DL}} - \frac{1}{e_0\underset{s}{L}}C_{\mathrm{E}}^{\mathrm{DL}} \cdot \frac{dU_{\mathrm{E}}^{\mathrm{DL}}}{dt} = \frac{e_0}{k_{\mathrm{B}}T}E_{\mathrm{A,E}}^T - \left(f_{\mathrm{A}} - f_{\mathrm{E}}\right) - \frac{1}{e_0\underset{s}{L}}i \qquad [53]$$

The term $e_0\underset{s}{L}$ can be considered as the *exchange current density*.[28]

Onsager coefficient of the intercalation reaction.—The Onsager coefficient $\underset{s}{L}$ (or the exchange current density $e_0\underset{s}{L}$) of the surface reaction 37 could in principle be a function of the surface chemical potentials (or surface concentrations), i.e. $\underset{s}{L} = \underset{s}{L}(\underset{s}{\mu}_{\mathrm{A}_C}, \underset{s}{\mu}_{\mathrm{E}_C}, \underset{s}{\mu}_{\mathrm{E}_S}, \underset{s}{\mu}_{\mathrm{A}_e})$ or $\underset{s}{L} = \underset{s}{L}(\underset{s}{\lambda})$ or the surface affinity, i.e. $\underset{s}{L} = \underset{s}{L}(\underset{s}{\lambda})$, as long as the condition $\underset{s}{L} > 0$ is ensured.[4,8,26] Note, however, that surface thermodynamics dictates the dependency of $\underset{s}{L}$ on the surface chemical potentials $\underset{s}{\mu}_\alpha$ and not the bulk chemical potentials μ_α.

For a general relation $\underset{s}{L} = \underset{s}{L}(\underset{s}{\mu}_{\mathrm{A}_C}, \underset{s}{\mu}_{\mathrm{E}_C}, \underset{s}{\mu}_{\mathrm{E}_S})$ we can *pull back* the surface chemical potentials $\underset{s}{\mu}_\alpha$ through the double layer to obtain

$$\underset{s}{L} = \underset{s}{L}\left(\mu_{\mathrm{A}_C}(y_{\mathrm{A}_C}|_{\mathrm{AE}}), \mu_{\mathrm{E}_C}(y_{\mathrm{E}_C}|_{\mathrm{AE}}^{+}) - e_0 U_{\mathrm{E}}^{\mathrm{SCL}}, \mu_{\mathrm{E}_S}(y_{\mathrm{E}_S}|_{\mathrm{AE}}^{+})\right). \qquad [54]$$

Note that this necessarily restricts the functional dependency of $\underset{s}{L}$ on the mole fractions $y_\alpha|^{\mathrm{A,E}}$ at the interface $\Sigma_{\mathrm{A,E}}$.

Consider, for example a model $\underset{s}{L} = \underset{s}{L}_{\mathrm{E}}(y_{\mathrm{E}_C}|_{\mathrm{AE}}^{+})$, where the exchange current density is dependent on the electrolyte concentration at the interface. This would be, however, thermodynamically inconsistent since the general functional dependency of 54 requires for the electrolyte concentration at the interface

$$\underset{s}{L} = \underset{s}{L}_{\mathrm{E}}(\mu_{\mathrm{E}_C}(y_{\mathrm{E}_C}|_{\mathrm{AE}}^{+}) - e_0 U_{\mathrm{E}}^{\mathrm{SCL}}) = \hat{\underset{s}{L}}_{\mathrm{E}}(y_{\mathrm{E}_C}|_{\mathrm{AE}}^{+} \cdot \mathrm{e}^{-\frac{e_0}{k_{\mathrm{B}}T}U_{\mathrm{E}}^{\mathrm{SCL}}}). \qquad [55]$$

Another commonly used model is a functional dependency of $\underset{s}{L}$ on the concentration $y_{\mathrm{A}_C}|_{\mathrm{AE}}$ of intercalated ions at the interface, i.e. $\underset{s}{L} = \underset{s}{L}_{\mathrm{A}}(y_{\mathrm{A}_C}|_{\mathrm{AE}})$. Since the space charge layer in the active particle $U_{\mathrm{A}}^{\mathrm{SCL}}$ is essentially constant (because $\underset{s}{\mu}_{\mathrm{A}_e}$ is constant), we can indeed write

$$\underset{s}{L} = \underset{s}{L}_{\mathrm{A}}\left(\mu_{\mathrm{A}_C}(y_{\mathrm{A}_C}|_{\mathrm{AE}})\right) = \hat{\underset{s}{L}}_{\mathrm{A}}(y_{\mathrm{A}_C}|_{\mathrm{AE}}). \qquad [56]$$

We discuss this aspect as well as various models for $\underset{s}{L}(\underset{s}{\mu}_{\mathrm{A}_C}, \underset{s}{\mu}_{\mathrm{E}_C}, \underset{s}{\mu}_{\mathrm{E}_S}, \underset{s}{\mu}_{\mathrm{A}_e})$ in Discussion of the exchange current density section. Meanwhile we assume $\underset{s}{L} = \text{const.}$ and proceed the following derivation and the discussion based on this assumption since it turns out to be very reasonable.

Discussion of the model parameters.—At this stage, it is illustrative to discuss the explicit value of the parameters.

- For the electrode geometry we consider for $\Sigma_{\mathrm{A,E}}$ a planar surface of area A and a thickness $d_{\mathrm{A}} = 10\,[\mu\mathrm{m}]$ which yields $V_{\mathrm{A}} = A \cdot d_{\mathrm{A}}$ and $x_{\mathrm{AE}} = 10\,[\mu\mathrm{m}]$. The electrolyte is considered with a thickness of $d_{\mathrm{E}} = 50\,[\mu\mathrm{m}]$. This corresponds to the cell dimensions of the cell MX-6 in Ref. 2.
- Throughout this work we consider DMC as solvent with $n_{\mathrm{E}_S}^R = 11.91\left[\frac{\mathrm{mol}}{\mathrm{L}}\right]$ and assume for the solvation number $\kappa_{\mathrm{E}} = 4$. The reference electrolyte concentration is $n_{\mathrm{E}}^R = 1\left[\frac{\mathrm{mol}}{\mathrm{L}}\right]$ and average amount of electrolyte is $\bar{n}_{\mathrm{E}}$ and a parameter of the model.
- Average concentrations (or mole fractions) are abbreviated as

$$\bar{y}_\alpha = \frac{1}{V_{\mathrm{E}}}\int_{\Omega_{\mathrm{E}}} y_\alpha \, dV \qquad \alpha = \mathrm{E}_C, \mathrm{E}_A, \mathrm{E}_S \qquad [57]$$

for the electrolyte species and

$$\bar{y}_{\mathrm{A}_C} = \frac{1}{V_{\mathrm{A}}}\int_{\Omega_{\mathrm{A}}} y_{\mathrm{A}_C} \, dV \qquad [58]$$

for the amount of intercalated ions in the active phase.

- For the active particle phase we consider $\mathrm{Li}(\mathrm{Ni}_{1/3}\mathrm{Mn}_{1/3}\mathrm{Co}_{1/3})\mathrm{O}_2$ (NMC) whereby

$$q_{\mathrm{A}}^{V,\mathrm{NMC}} = 1294\left[\frac{\mathrm{mA\,h}}{\mathrm{cm}^3}\right] \quad \text{and} \quad q_{\mathrm{A}}^{M,\mathrm{NMC}} = 318\left[\mathrm{mA\,h\,g}^{-1}\right] \qquad [59]$$

which is simply computed from the density and stoichiometry of the bulk material.[38] As parameters for the chemical potential μ_{A_C} we consider an occupation number of $\omega_{\mathrm{A}} = 10$ and a Redlich–Kister interaction energy of $\gamma_{\mathrm{A}} = 13$.[24]

- The differential capacity $C_{\mathrm{E}}^{\mathrm{DL}}$ has a prescribed value (actually $C_{\mathrm{E}}^{\mathrm{DL}}$ is a function of $U_{\mathrm{E}}^{\mathrm{SCL}}$, but we proceed here with a constant approximation for the sake of simplicity[9] of about

$$C_{\mathrm{E}}^{\mathrm{DL}} = 100\left[\frac{\mu\mathrm{F}}{\mathrm{cm}^2}\right] \qquad [60]$$

[b]Note again that $U_{\mathrm{AE}}^{\mathrm{DL}} = U_{\mathrm{E}}^{\mathrm{SCL}} - U_{\mathrm{A}}^{\mathrm{SCL}}$ and that the space charge layer drop $U_{\mathrm{A}}^{\mathrm{SCL}}$ is constant due to the material model $\underset{s}{\mu}_{\mathrm{A}_e} = \text{const.}$ whereby $\frac{dU_{\mathrm{E}}^{\mathrm{SCL}}}{dt} = \frac{dU_{\mathrm{AE}}^{\mathrm{DL}}}{dt}$.

- The electrode capacity Q is

$$Q = \int_{\Omega_{\mathrm{A}}} q_{\mathrm{A}}^V \cdot y_{\mathrm{A}_C}\, dV = Q_{\mathrm{A}}^V \cdot \bar{y}_{\mathrm{A}_C} \quad \text{with} \quad Q_{\mathrm{A}}^V := V_{\mathrm{A}} \cdot q_{\mathrm{A}}^V \qquad [61]$$

This yields the non-dimensional **capacity**

$$\frac{Q}{Q_{\mathrm{A}}^V} = \bar{y}_{\mathrm{A}_C} \in (0, 1) \qquad [62]$$

which is sometimes also called *status of charge* (SOC) or *depth of discharge* (DOD).

Note that during *discharge* of a complete battery the cathode is actually filled up with lithium. In a half cell with metallic lithium as counter electrode, *discharge* thus actually means *filling up* the intercalation electrode, here the NMC cathode material. Hence $Q/Q_{\mathrm{A}}^V \to 0$ corresponds to a fully charged cathode (i.e. no lithium in the intercalation compound, $\bar{y}_{\mathrm{A}_C} \to 0$) while $Q/Q_{\mathrm{A}}^V \to 1$ corresponds to a fully discharged cathode (i.e. the intercalation compound is completely filled with lithium, $\bar{y}_{\mathrm{A}_C} \to 1$).

- From the charge balance 35 of the active particle we can deduce

$$Q = Q^0 + \int_0^t I(t')dt \quad \text{with} \quad Q^0 = \int_{\Omega_{\mathrm{A}}} q_{\mathrm{A}}^V \cdot y_{\mathrm{A}_C}(\mathbf{x}, t = 0)\, dV \qquad [63]$$

where I is the current flowing into the intercalation electrode during *discharge* and $Q(t = 0)$ the initial charge state. For a galvanostatic discharge $I > 0$ we obtain thus

$$Q = Q^0 + I \cdot t. \qquad [64]$$

- The C-Rate C_h [1] defines (implicitly) the current at which after h-hours the intercalation cathode is completely filled during galvanostatic discharge. C_1 is thus the rate at which the battery is charged within one hour and commonly abbreviated just as C-rate C, i.e.

$$I_C = \frac{Q_{\mathrm{A}}^V}{1\,[\mathrm{h}]} = A\frac{d_{\mathrm{A}} \cdot q_{\mathrm{A}}^V}{1\,[\mathrm{h}]}. \qquad [65]$$

We can hence express the current I in multiples of the C-rate, i.e.

$$I = C_h \cdot I_C \qquad [66]$$

which yields

$$Q = Q^0 + I \cdot t = Q^0 + C_h \cdot I_C \cdot t = Q^0 + C_h \cdot \frac{Q_{\mathrm{A}}^V}{1\,[\mathrm{h}]} \cdot t = Q_{\mathrm{A}}^V (y_{\mathrm{A}_C}^0 + C_h \frac{t}{[\mathrm{h}]}) \qquad [67]$$

The only parameter for the current density $i = I/A$ is thus C_h.

- For the time t we consider the interval of one discharge cycle, i.e. $t \in [0, t_{\mathrm{end}}]$ with

$$t_{\mathrm{end}} = \frac{1\,[h]}{C_h} \qquad [68]$$

We can thus introduce the non-dimensional time

$$\tau := C_h \frac{t}{3600\,[s]} \in [0, 1] \qquad [69]$$

whereby the capacity rewrites as

$$Q/Q_{\mathrm{A}}^V = (y_{\mathrm{A}_C}^0 + \tau). \qquad [70]$$

- For the current density i at the planar electrode we have thus

$$i = \frac{I}{A} = \frac{C_h \cdot I_C}{A} = i_{\mathrm{A}}^C \cdot C_h \quad \text{with} \quad i_{\mathrm{A}}^C := \frac{d_{\mathrm{A}} \cdot q_{\mathrm{A}}^V}{1\,[\mathrm{h}]}. \qquad [71]$$

Discussion of the scaling.—Consider the non-dimensional voltage

$$\widetilde{U} = \frac{e_0}{k_{\mathrm{B}}T} U_{\mathrm{E}}^{\mathrm{SCL}} \qquad [72]$$

and abbreviate

$$\widetilde{H} = \frac{e_0}{k_{\mathrm{B}}T} E_{\mathrm{A,R,E}} - f_{\mathrm{A}} + f_{\mathrm{E}} \qquad [73]$$

which yields

$$\widetilde{U} - c_1 \cdot \frac{C_h}{\widetilde{L}} \cdot \frac{d\widetilde{U}}{d\tau} = \widetilde{H}(1 - \tau) - \frac{C_h}{\widetilde{L}} \qquad [74]$$

with

$$c_1 := \frac{1}{d \cdot q_{\mathrm{A}}^V} C_{\mathrm{E}}^{\mathrm{DL}} \frac{k_{\mathrm{B}}T}{e_0} \qquad [75]$$

The parameters $d_{\mathrm{A}} = 0.01$ [cm] and $q_{\mathrm{A}}^V = 1294\left[\mathrm{mA\,h\,cm^{-3}}\right]$ yield

$$d_{\mathrm{A}} \cdot q_{\mathrm{A}}^V = 0.01\,[\mathrm{cm}] \cdot 1294\left[\mathrm{mA\,h\,cm^{-3}}\right] \cdot \frac{1}{[\mathrm{h}]} = 12.94\left[\frac{\mathrm{mA\,h}}{\mathrm{cm^2}}\right] \qquad [76]$$

and

$$C_{\mathrm{E}}^{\mathrm{DL}} \frac{k_{\mathrm{B}}T}{e_0} = 100\left[\frac{\mu\mathrm{F}}{\mathrm{cm^2}}\right] \cdot 0.0257\,[\mathrm{V}] = 2.568\left[\frac{\mu\mathrm{C}}{\mathrm{cm^2}}\right] \qquad [77]$$

whereby

$$c_1 = 5.51 \cdot 10^{-8}. \qquad [78]$$

The double layer contribution in Eq. 51 is thus almost negligible whereby 51 reduces to

$$i = -e_0 L_s g\left(\frac{1}{k_{\mathrm{B}}T}\lambda_s\right). \qquad [79]$$

We consider for the exchange current density the rescaling

$$e_0 L_s = \widetilde{L} \cdot i_{\mathrm{A}}^C = \widetilde{L}\frac{d_{\mathrm{A}} \cdot q_{\mathrm{A}}^V}{1\,[\mathrm{h}]}. \qquad [80]$$

This is the crucial decomposition throughout this work and $\widetilde{L}$ the parameter of the surface reaction rate R.

For the current density $i = i_{\mathrm{A}}^C \cdot C_h^s$ and the inverse function g^{-1} we obtain thus with Eq. 48 for the surface affinity λ_s the general expression

$$E = E_{\mathrm{A,C}} - \frac{k_{\mathrm{B}}T}{e_0}\left(f_{\mathrm{A}} - f_{\mathrm{E}}|_{\mathrm{AE}} + f_{\mathrm{E}}|_{\mathrm{EC}}\right) + \frac{k_{\mathrm{B}}T}{e_0} g^{-1}\left(-\frac{C_h}{\widetilde{L}}\right) - U_{\mathrm{A}}^{\mathrm{bulk}} + U_{\mathrm{E}}^{\mathrm{bulk}} \qquad [81]$$

for the cell voltage E.

Discussion

Throughout the manuscript, we assume that the initial state is completely uncharged, i.e. $Q^0 = 0$ and $y_{\mathrm{A}_C}^0 = 0$. If not stated otherwise, we abbreviate

$$y_{\mathrm{A}_C} = y_{\mathrm{A}} \quad \text{and} \quad y_{\mathrm{E}_C} = y_{\mathrm{E}} \qquad [82]$$

as well as the respective densities $n_{\mathrm{A}_C} = n_{\mathrm{A}}, n_{\mathrm{E}_C} = n_{\mathrm{E}}$, fluxes $\mathbf{J}_{\mathrm{A}_C} = \mathbf{J}_{\mathrm{A}}, \mathbf{J}_{\mathrm{E}_C} = \mathbf{J}_{\mathrm{E}}$, and chemical potential $\mu_{\mathrm{A}_C} = \mu_{\mathrm{A}}$ in the following.

We seek to discuss the general relation 81 of the cell voltage E as function of the capacity

$$\frac{Q}{Q_{\mathrm{A}}^V} = \bar{y}_{\mathrm{A}} \in (0, 1) \qquad [83]$$

during discharge of an intercalation electrode. Note that necessarily $C_h > 0$ (discharge) and $\widetilde{L} > 0$ (Onsager constraint of 38), whereby $g^{-1}\left(-\frac{1}{2}\frac{C_h}{\widetilde{L}}\right) < 0$, which entails that any current decreases the cell voltage E during discharge.

We will discuss consecutively the following hierarchy of approximations:

BV 0: infinite slow discharge - the open circuit potential
BV 1: infinite fast diffusion and conductivity in the active particle and the electrolyte
BV 2: finite conductivity in the active particle, infinite diffusion in the active particle, infinite fast diffusion and conductivity the electrolyte
BV 3: finite conductivity and diffusion in the active particle, infinite fast diffusion and conductivity the electrolyte

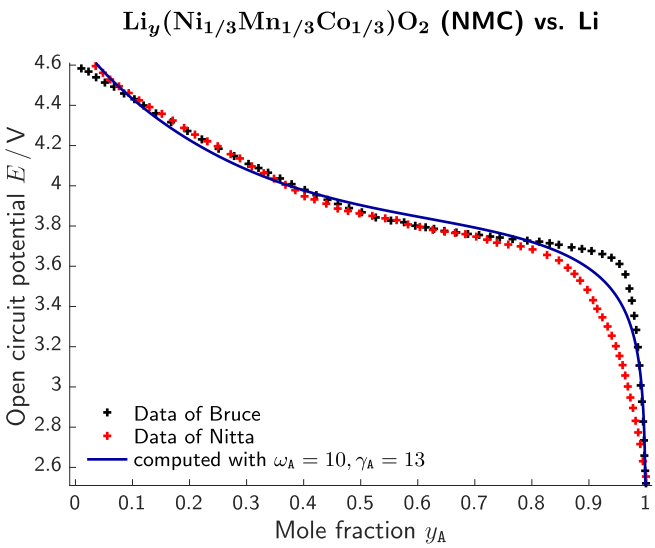

Figure 4. OCP of $Li_y(Ni_{1/3}Mn_{1/3}Co_{1/3})O_2$. Comparison between the material model 11 and experimental data of P. Bruce (Data of Fig. 3 in Ref. 39) and N. Nitta et al. (Data of Fig. 4e in Ref. 52).

BV 4: finite conductivity and diffusion in the active particle, finite conductivity in the electrolyte, infinite fast diffusion the electrolyte

BV 5: finite conductivity in the active particle and the electrolyte, finite solid state diffusion in the intercalation electrode as well as finite diffusion in the electrolyte

BV 0: Open circuit potential.—The open circuit potential (OCP) is obtained from 81 as

$$E = \frac{1}{e_0}\left(\mu_{C_C} - \mu_A(y_A)\right) \qquad [84]$$

for $C_h = 0$ (infinite slow discharge), which entails also $U_A^{bulk} = U_E^{bulk} = 0$ as well as $y_E|_{AE} = y_E|_{EC}$. Hence we have

$$E = E_{A,C} - \frac{k_B T}{e_0} f_A(\bar{y}_A) = E^{(0)}(Q/Q_A^V). \qquad [85]$$

For $Li_y(Ni_{1/3}Mn_{1/3}Co_{1/3})O_2$[39] as intercalation electrode, the two parameters of the chemical potential function μ_A are the occupation number $\omega_A = 10$ and the interaction energy $\gamma_A = 13$ of the Redlich–Kister type enthalpy contribution. This yields an absolute ℓ^2-error of 0.064 / V and a relative error of 1.860% vs. experimental data of P. Bruce et al.,[39] and Fig. 4 shows a comparison to two experimental data sets of measured OCP data.

BV 1: Infinite fast diffusion and conductivity in the active particle and the electrolyte.—Infinite conductivity within the active particle phase as well as within the electrolyte yields

$$U_A^{bulk} = 0 \quad \text{and} \quad U_E^{bulk} = 0. \qquad [86]$$

and infinite fast diffusion in the active particle and the electrolyte entails

$$y_A(x,t) = \text{const. } w.r.t.x \quad \text{and} \quad y_E(x,t) = \text{const. } w.r.t.x. \qquad [87]$$

Hence $y_A|_{AE}$ is directly related to the capacity via

$$y_A|_{AE} = \bar{y}_A = Q/Q_A^V \qquad [88]$$

whereby the cell voltage of **BV 1** is

$$E = E_{A,C} - \frac{k_B T}{e_0} f_A(\bar{y}_A) + \frac{k_B T}{e_0} g^{-1}\left(-\frac{C_h}{\widetilde{L}}\right) =: E^{(1)}(Q/Q_A^V; C_h, \widetilde{L}). \qquad [89]$$

It is a simple algebraic relation between the measured cell voltage E, the C-rate C_h, the capacity Q and the (non-dimensional) exchange current density $\widetilde{L}$.

In order to compare the cell voltage E computed in the approximation **BV 1** with other approximations, we abbreviate the voltage computed from 89 as $E^{(1)}$. Note that cell voltage 89 is actually *independent* of the electrolyte. For $\widetilde{L} = 1$ we obtain the voltage/capacity relation given in Fig. 5 for a variation of C_h from 0 (open circuit potential) to $C_h = 100$ (extremely fast discharge).

Reaction overpotential.—We define the *reaction overpotential* as

$$\eta^R = E^{(0)} - E^{(1)} = -\frac{k_B T}{e_0} g^{-1}\left(-\frac{C_h}{\widetilde{L}}\right) \qquad [90]$$

which is actually independent of the status of charge or capacity. Measured voltage data $\check{E} = \check{E}(C_h)$ would thus allow to determine $\widetilde{L}$ and the parameter $\alpha \in (0, 1)$.

Fig. 6 shows computations of the reaction overpotential η^R for various values of α and $\widetilde{L}$ as function of C_h.

BV 2: Contribution of finite active phase conductivity.—Finite conductivity within active particle phase entails from Eq. 35

$$U_A^{bulk} = R_A^{bulk} \cdot i \quad \text{with} \quad R_A^{bulk} = \frac{d_A}{\sigma_A}. \qquad [91]$$

Employing the scaling 71 of the current density i, i.e. $i = i_A^C \cdot C_h$, as well as the decomposition

$$\sigma_A = \sigma_A^C \cdot \widetilde{\sigma}_A \quad \text{with} \quad \sigma_A^C := d_A \cdot i_A^C \cdot \frac{e_0}{k_B T} = \frac{d_A^2 q_A^V}{1\,[h]} \cdot \frac{e_0}{k_B T} \qquad [92]$$

yields

$$U_A^{bulk} = \frac{k_B T}{e_0} \frac{C_h}{\widetilde{\sigma}_A}. \qquad [93]$$

The quantity σ_A^C is the specific conductivity of the active particle phase at C-rate of one. For the parameters given in Discussion of the model parameters section σ_A^C computes as

$$\sigma_A^C \approx 4.9 \left[\frac{\text{mS}}{\text{cm}}\right]. \qquad [94]$$

The measured cell voltage is then

$$\begin{aligned} E &= E_{A,C} - \frac{k_B T}{e_0}\left(f_A(\bar{y}_A) - g^{-1}\left(-\frac{C_h}{\widetilde{L}}\right) + \frac{C_h}{\widetilde{\sigma}_A}\right) \\ &=: E^{(2)}(Q/Q_A^V; C_h, \widetilde{L}, \widetilde{\sigma}_A) \end{aligned} \qquad [95]$$

which is (yet again) a simple algebraic relation between E, the C-rate C_h, and the capacity Q/Q_A^V. $E^{(2)}$ is additionally parametrically dependent on the conductivity $\widetilde{\sigma}_A$.

We define the active phase conductivity overpotential η_A^σ as

$$\eta_A^\sigma := E^{(1)} - E^{(2)} = \frac{k_B T}{e_0} \frac{C_h}{\widetilde{\sigma}_A}. \qquad [96]$$

BV 3: Contribution of the solid-state diffusion in the active particle phase.—*Constant diffusion coefficient.*—Reconsider that we have assumed yet y_A = const. with respect to space in the intercalation particle. In general, however, we have to solve a (here 1D) diffusion equation

$$\frac{\partial n_A}{\partial t} = -\partial_x j_A \quad \text{with} \quad j_A = -D_A n_A \partial_x f_A(y_A) \qquad [97]$$

with

$$j_A\big|_{x=0}^{+} = 0 \quad \text{and} \quad j_A\big|_{AE}^{-} = -\frac{1}{e_0} i. \qquad [98]$$

This yields at the interface $\Sigma_{A,E}$ some solution

$$y_A(x,t)\big|_{x=x_{AE}} = y_A|_{AE}(t; i) \qquad [99]$$

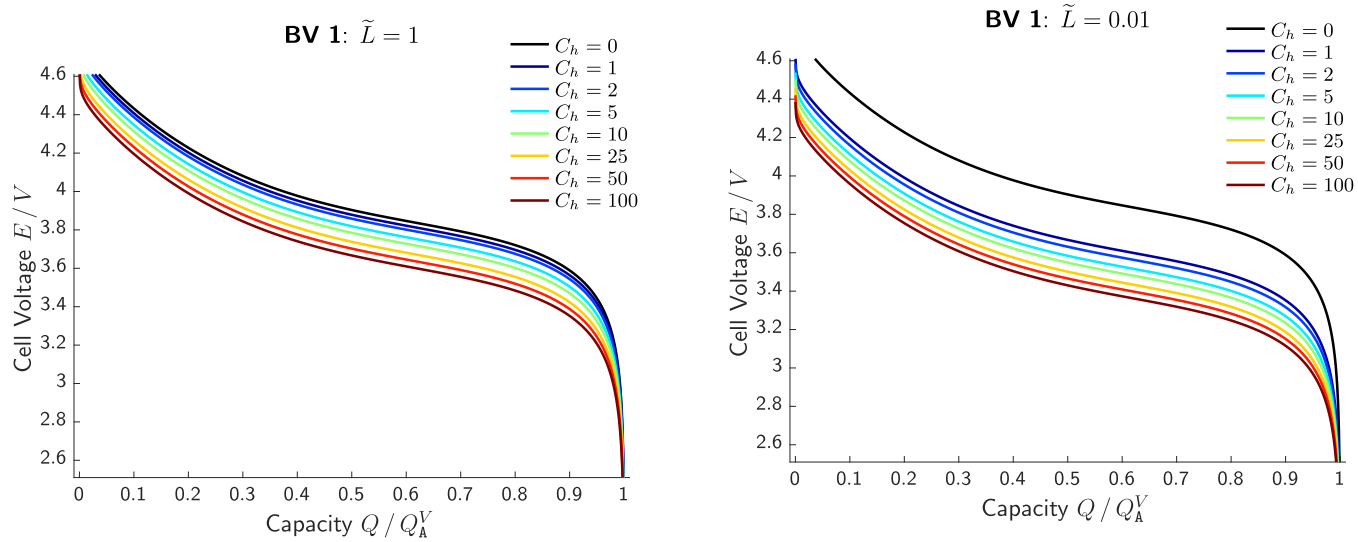

Figure 5. Computed voltage E as function of the capacity Q/Q_{A} according to Eq. 89 for various values of $\widetilde{L}$ and C_h.

which will also impact the cell voltage

$$E = E_{\mathrm{A,C}} - \frac{k_{\mathrm{B}}T}{e_0}\left(f_{\mathrm{A}}(y_{\mathrm{A}}|_{\mathrm{AE}}(t;i)) - g^{-1}\left(-\frac{C_h}{\widetilde{L}}\right) + \frac{C_h}{\widetilde{\sigma}_{\mathrm{A}}}\right) \quad [100]$$

$$=: E^{(3)}(Q/Q_{\mathrm{A}}^V; C_h, \widetilde{L}, \widetilde{\sigma}_{\mathrm{A}}, \widetilde{D}_{\mathrm{A}}) \quad [101]$$

In order to discuss this impact systematically, we apply the following scaling

$$\tau = C_h \frac{t}{[h]} \in [0,1] \quad \text{and} \quad \xi = \frac{x}{d_{\mathrm{A}}} \in [0,1] \quad [102]$$

as well as

$$n_{\mathrm{A}} = y_{\mathrm{A}} \cdot \frac{q_{\mathrm{A}}^V}{e_0} \quad \text{and} \quad \widetilde{j}_{\mathrm{A}} = \frac{1}{\underset{s}{L}} j_{\mathrm{A}} \quad [103]$$

which leads to

$$\frac{C_h}{\widetilde{L}}\frac{\partial y_{\mathrm{A}}}{\partial t} = -\partial_\xi \widetilde{j}_{\mathrm{A}}. \quad [104]$$

The dimensionless flux

$$\widetilde{j}_{\mathrm{A}} = \frac{1}{\widetilde{L}} j_{\mathrm{A}} = -\frac{1}{\widetilde{L}}\frac{1\,[\mathrm{h}]}{d_{\mathrm{A}}^2} D_{\mathrm{A}} y_{\mathrm{A}} \partial_\xi f_{\mathrm{A}}(y_{\mathrm{A}}) \quad [105]$$

yields the dimensionless diffusion coefficient

$$\widetilde{D}_{\mathrm{A}} = \frac{1\,[\mathrm{h}]}{d_{\mathrm{A}}^2} D_{\mathrm{A}} \quad [106]$$

and thus

$$\widetilde{j}_{\mathrm{A}} = -\frac{\widetilde{D}_{\mathrm{A}}}{\widetilde{L}} y_{\mathrm{A}} \partial_\xi f_{\mathrm{A}}(y_{\mathrm{A}}). \quad [107]$$

At the interface $\Sigma_{\mathrm{A,E}}$ we have thus

$$\widetilde{j}_{\mathrm{A}}\big|_{\xi=1} = -\frac{C_h}{\widetilde{L}}. \quad [108]$$

Overall we may write

$$\frac{C_h}{\widetilde{D}_{\mathrm{A}}}\frac{\partial y_{\mathrm{A}}}{\partial \tau} = \partial_\xi\left(y_{\mathrm{A}}\frac{\partial f_{\mathrm{A}}}{\partial y_{\mathrm{A}}}\partial_\xi y_{\mathrm{A}}\right) \quad [109]$$

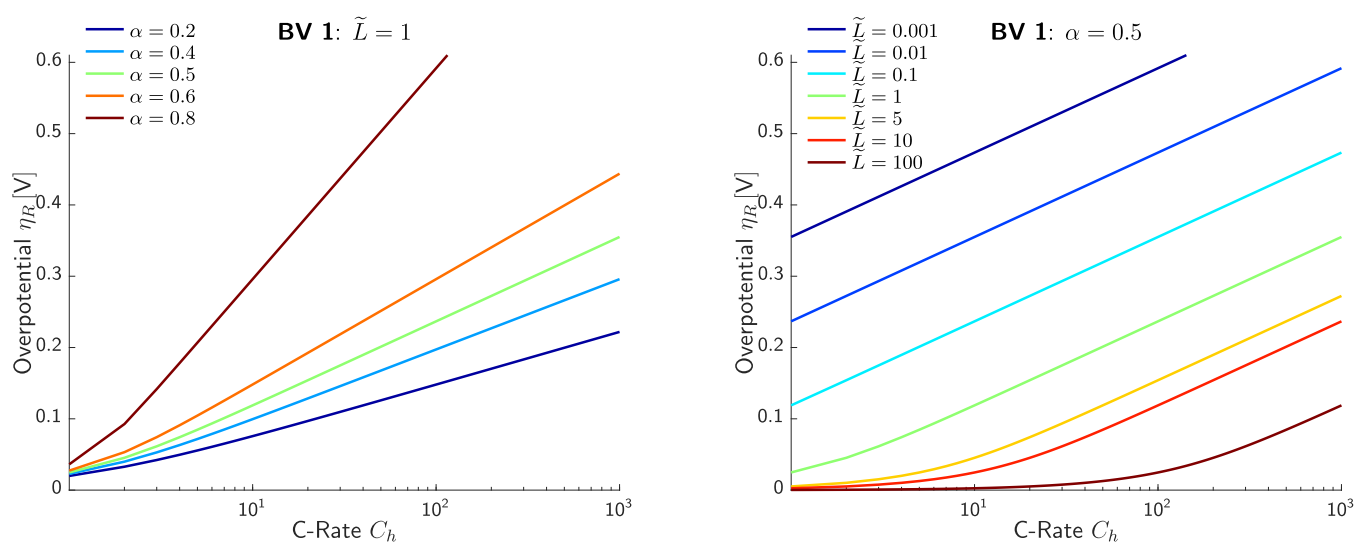

Figure 6. Reaction overpotential η^R as function of the C-Rate C_h with parameter variations of α and $\widetilde{L}$.

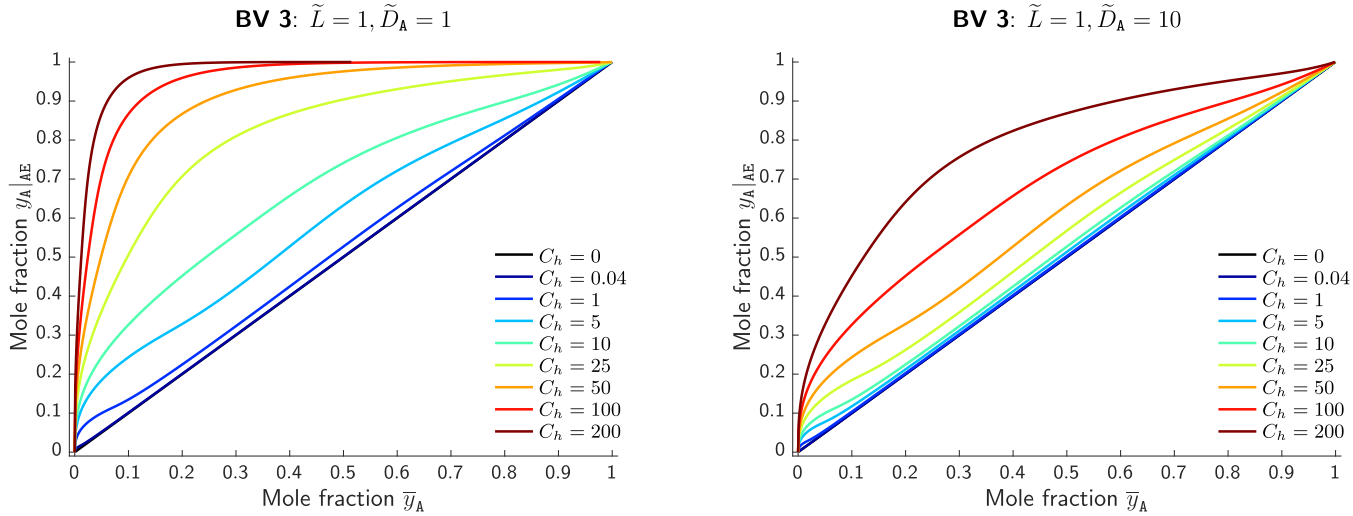

Figure 7. Concentration $y_{\mathrm{A}}\big|_{\mathrm{AE}} = \hat{y}_{\mathrm{A}}|_{\mathrm{AE}}$ of intercalated ions at the interface $\Sigma_{\mathrm{A,E}}$ as function the status of discharge Q/Q_{A}^{V} for various values of C_h and $\widetilde{D}_{\mathrm{A}}$.

with

$$y_{\mathrm{A}} \frac{\partial f_{\mathrm{A}}}{\partial y_{\mathrm{A}}} \partial_{\xi} y_{\mathrm{A}}\big|_{\xi=0} = 0 \quad \text{and} \quad y_{\mathrm{A}} \frac{\partial f_{\mathrm{A}}}{\partial y_{\mathrm{A}}} \partial_{\xi} y_{\mathrm{A}}\big|_{\xi=1} = \frac{C_h}{\widetilde{D}_{\mathrm{A}}}. \qquad [110]$$

Note that we can analytically compute $y_{\mathrm{A}} \frac{\partial f_{\mathrm{A}}}{\partial y_{\mathrm{A}}} = \Gamma_{\mathrm{A}}^{\mathrm{tf}}(y_{\mathrm{A}})$ from Eq. 11 (see also appendix B1) as

$$\Gamma_{\mathrm{A}}^{\mathrm{tf}} = y_{\mathrm{A}} \cdot \frac{\partial f_{\mathrm{A}}}{\partial y_{\mathrm{A}}} = \frac{1}{(1-y_{\mathrm{A}})(\frac{1}{\omega_{\mathrm{A}}} y_{\mathrm{A}} + (1-y_{\mathrm{A}}))}$$
$$+ \gamma_{\mathrm{A}} \cdot \left(16 \cdot y_{\mathrm{A}}^3 - 22 y_{\mathrm{A}}^2 + \frac{25}{3} y_{\mathrm{A}}\right). \qquad [111]$$

Since the problem 109 is non-linear, a classical separation *Ansatz* $y_{\mathrm{A}} = X(\xi) \cdot T(\tau)$ is not meaningful. We proceed thus with solving the problem 109 with 110 numerically with MATLAB and the pdepe() function. The syntax for pdepe() of the problem 109 with 110 is given in appendix B2.

Based on the numerical solution $\hat{y}_{\mathrm{A}}(\xi, \tau)$ we compute then $y_{\mathrm{A}}\big|_{\mathrm{AE}} = \hat{y}_{\mathrm{A}}(\xi, \tau)|_{\xi=1}(\tau; C_h, \widetilde{D}_{\mathrm{A}})$ numerically for various values of C_h and $\widetilde{D}_{\mathrm{A}}$. The (global) capacity is yet $Q/Q_{\mathrm{A}}^{V} = \overline{y}_{\mathrm{A}} = \tau$.

We assume the same parameters as before, now additionally with two values of the diffusion coefficient $\widetilde{D}_{\mathrm{A}}$, i.e. slow diffusion $\widetilde{D}_{\mathrm{A}} = 1$ and fast diffusion $\widetilde{D}_{\mathrm{A}} = 10$, and compute $y_{\mathrm{A}}\big|_{\mathrm{AE}}$ as function of the capacity Q/Q_{A}^{V} (or time τ). Fig. 7 shows computations of $y_{\mathrm{A}}|_{\mathrm{AE}}$ for various discharge rates and diffusion coefficients in the active particle phase as function of the cell capacity. The angle bisection in black corresponds to the open circuit potential situation, where $y_{\mathrm{A}}|_{\mathrm{AE}} = \overline{y}_{\mathrm{A}}$. For increasing discharge rates, the concentration $y_{\mathrm{A}}|_{\mathrm{AE}}$ at the interface $\Sigma_{\mathrm{A,E}}$ is larger than the average concentration $\overline{y}_{\mathrm{A}}$ in Ω_{A} since the evacuation of intercalated ions is delayed by the finite diffusion. This effect becomes even stronger for smaller values of $\widetilde{D}_{\mathrm{A}}$, i.e. slow diffusion in the active particle.

The cell voltage E is then computed *a posteriori* from 100 based on the numerical solution of $y_{\mathrm{A}}|_{\mathrm{AE}}$. Fig. 8 displays the cell voltage for various discharge rates as well as slow ($\widetilde{D}_{\mathrm{A}} = 1$) and fast ($\widetilde{D}_{\mathrm{A}} = 10$) diffusion in the intercalation phase. Finite diffusion in the active particle has an enormous impact on the cell voltage and changes qualitatively the shape due to the non-linear feedback. This effect is also found experimentally, see Fig. 1, and extremely important since it determines the maximum amount of charge that can be withdrawn from an intercalation electrode.

Two important measures serve to discuss the impact of the diffusion coefficient $\widetilde{D}_{\mathrm{A}}$,

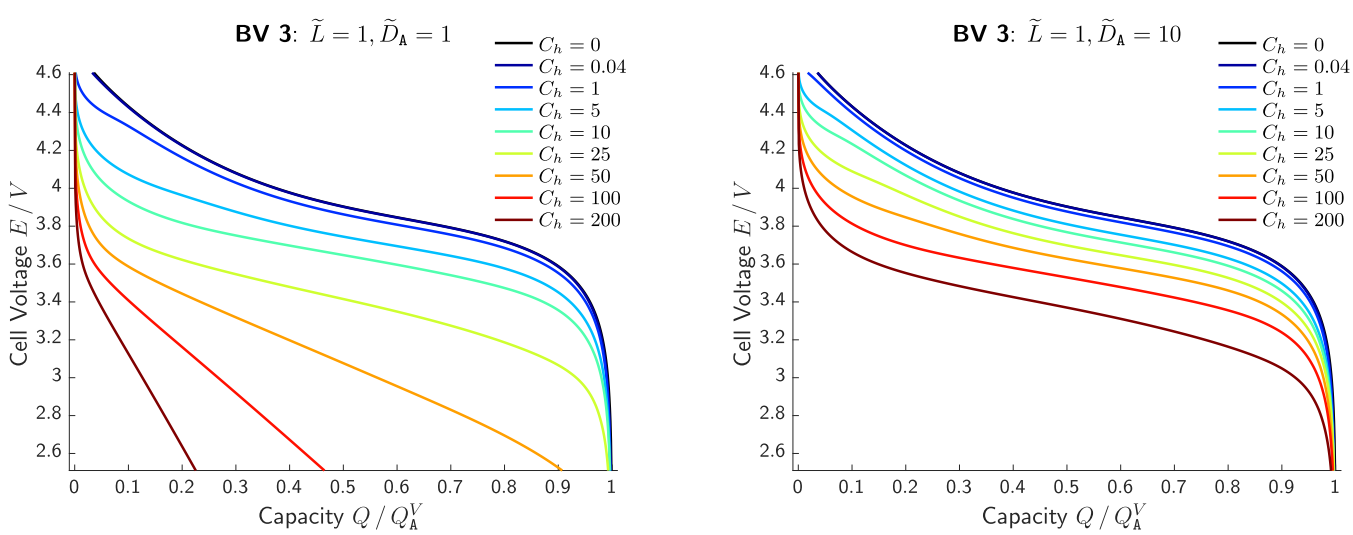

Figure 8. Cell voltage E for **BV 3** as function of the status of discharge for various values of C_h and $\widetilde{D}_{\mathrm{A}}$ with numerical computation of $\hat{y}_{\mathrm{A},0}(i)$ from the PDE 109 with boundary conditions 110.

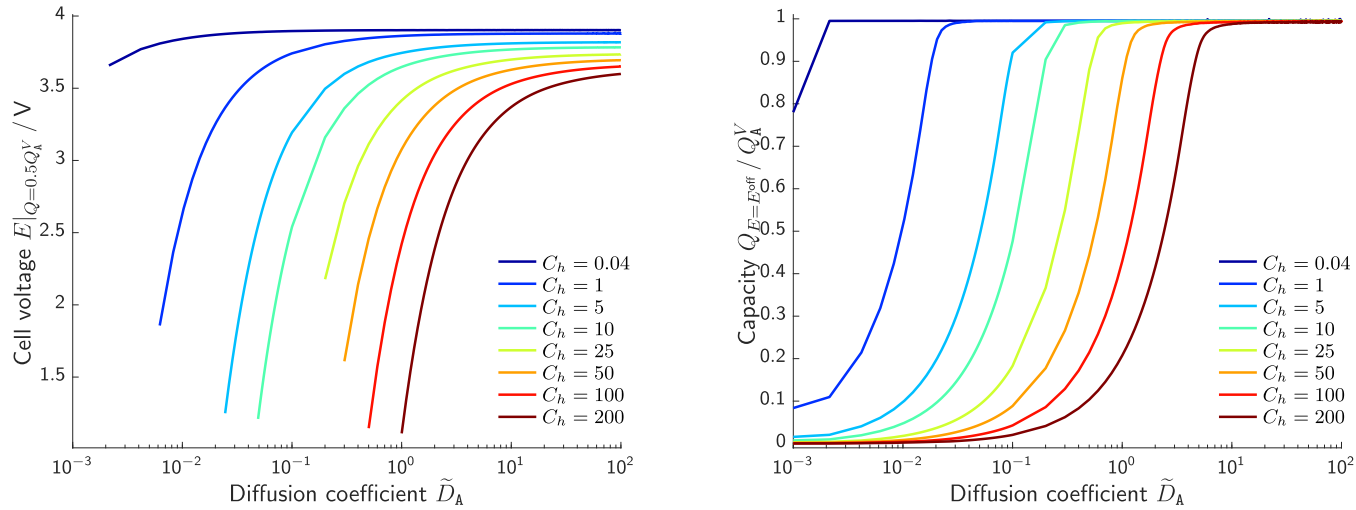

Figure 9. Cell voltage and Capacity for various discharge rates and diffusion coefficients. (a) Cell voltage at 50% state of discharge. (b) Capacity at the cutoff voltage $E^{\text{off}} = 2.6$/V.

- the cell voltage at 50% discharge, i.e. $E\big|_{Q=0.5\cdot Q_A^V}$,
- and the capacity $Q\big|_{E=E^{\text{off}}}$ at the cut off voltage E^{off}, here with $E^{\text{off}} = 2.6\,/\,\text{V}$.

Fig. 9 shows numerical computations of $E\big|_{Q=0.5\cdot Q_A^V}$ and $Q\big|_{E=E^{\text{off}}}$ for various values of the C-rate C_h and diffusion coefficients $\widetilde{D}_A$ in the range of $10^{-3} - 10^2$. For slow discharge rates, i.e. $C_h < 1$ a diffusion coefficient of $\widetilde{D}_A = 0.1$ is sufficient to achieve a voltage of $3\,/\,\text{V}$ at 50% discharge and capacity of 90% at the the cutoff voltage. However, for higher C-rates, e.g. $C_h = 50$, the impact of the solid state diffusion becomes enormous, **requiring** a diffusion coefficient of $\widetilde{D}_A > 0.3$ to discharge the electrode to 50%.

Overpotential η_A^D.—The *overpotential* due to finite diffusion in the active particle phase can be defined as

$$\eta_A^D := E^{(2)} - E^{(3)} \qquad [112]$$

which computes as

$$\eta_A^D = -\frac{k_B T}{e_0}\big(f_A(\bar{y}_A) - f_A(\hat{y}_A|_{AE})\big). \qquad [113]$$

Fig. 10 shows computations of η_A^D for slow and fast diffusion.

Concentration dependent diffusion coefficient.—The diffusion coefficient D_A in 34 was yet assumed to be a constant[c] with respect to the mole fraction y_A of intercalated ions in the solid phase. This assumption might be inappropriate or over-simplified, and we seek to discuss this hypothesis again on the cell voltage E as function the capacity Q and the C-rate C. For this sake, we consider in the following a concentration dependent diffusion coefficient

$$D_A = (1 - y_A)\cdot \hat{D}_A, \qquad [114]$$

where the constant $\hat{D}_A$ is scaled equally than before, yielding again dimensionless diffusion coefficient $\widetilde{D}_A = \frac{1[h]}{d_A^2}\hat{D}_A$. The term $(1 - y_A)$ models that the diffusion on a lattice reduces when the lattice becomes more occupied (i.e. $y_A \to 1$).

We obtain hence the non-dimensionalized transport equation

$$\frac{C_h}{\widetilde{D}_A}\frac{\partial y_A}{\partial \tau} = \partial_\xi\big((1 - y_A)\cdot y_A \frac{\partial f_A}{\partial y_A}\partial_\xi y_A\big) \qquad [115]$$

with boundary conditions

$$(1 - y_A)\cdot y_A \frac{\partial f_A}{\partial y_A}\partial_\xi y_A\big|_{\xi=0} = 0 \quad \text{and} \quad y_A \frac{\partial f_A}{\partial y_A}\partial_\xi y_A\big|_{\xi=1} = \frac{C_h}{\widetilde{D}_A}. \qquad [116]$$

[c]Note, however, that the *effective* diffusion coefficient $D_A \cdot \Gamma_A^{tf}$ as pre-factor of $\partial_x y_A$ in the flux relation 34 is inherently concentration dependent.

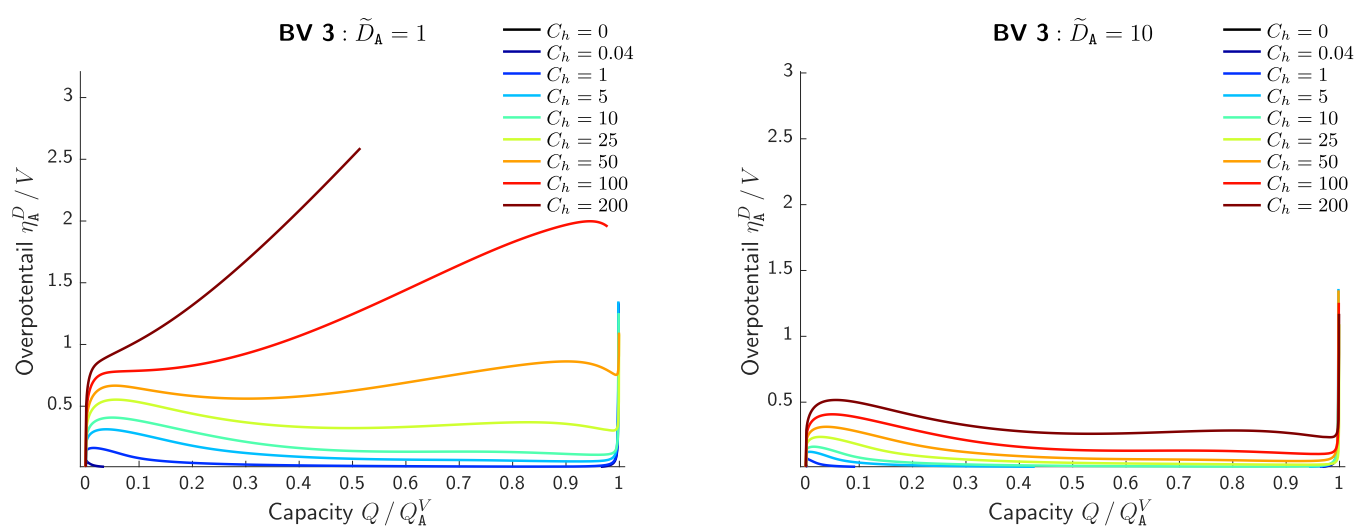

Figure 10. Overpotential η_A^D as function of the status of discharge Q/Q_A^V for slow ($\widetilde{D}_A = 1$) and fast ($\widetilde{D}_A = 10$) diffusion in the intercalation phase.

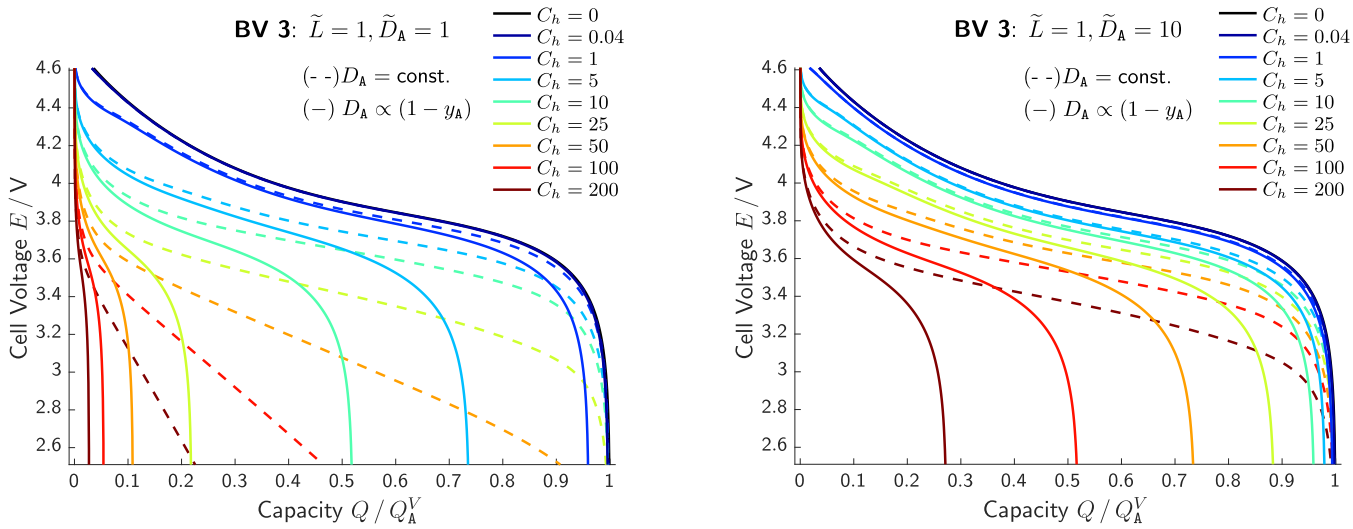

Figure 11. Cell voltage E for **BV 3** as function of the status of discharge for various values of C_h and $\widetilde{D}_{\mathrm{A}}$ with numerical computation of $\hat{y}_{\mathrm{A},0}(i)$ for a constant diffusion coefficient (PDE 109 with boundary conditions 110) and a concentration dependent diffusion coefficient (PDE 115 with boundary condition 116).

This equation system is again solved numerically with MATLAB and the pdepe() function yielding numerical solutions $\hat{y}_{\mathrm{A}}(\xi, \tau)$ whereby we compute then $y_{\mathrm{A}}\big|_{\mathrm{AE}} = \hat{y}_{\mathrm{A}}(\xi, \tau)|_{\xi=1}(\tau; C_h, \widetilde{D}_{\mathrm{A}})$ for various values of C_h and $\widetilde{D}_{\mathrm{A}}$. The (global) capacity is yet $Q/Q_{\mathrm{A}}^V = \bar{y}_{\mathrm{A}} = \tau$. The cell voltage E is then computed *a posteriori* from 100 based on the numerical solution of $y_{\mathrm{A}}|_{\mathrm{AE}}$.

We assume the same parameters as before and two values of the diffusion coefficient $\widetilde{D}_{\mathrm{A}}$, i.e. slow diffusion $\widetilde{D}_{\mathrm{A}} = 1$ and fast diffusion $\widetilde{D}_{\mathrm{A}} = 10$. Based on the numerical solution of 115 and 116 we compute $y_{\mathrm{A}}\big|_{\mathrm{AE}}$ as function of the capacity Q/Q_{A}^V (or time τ), and subsequent the cell voltage E from 100 based on the numerical solution of $y_{\mathrm{A}}|_{\mathrm{AE}}$.

Fig. 11 displays the cell voltage for various discharge rates computed numerically with a constant (dashed line) and the concentration dependent (solid line) diffusion coefficient according to 114.

Expectably, the two models behave similar when the intercalation electrode is empty, i.e. y_{A} close zero. However, when the electrode gets filled with lithium (i.e. $y_{\mathrm{A}} \to 1$), the $(1-y_{\mathrm{A}})$-term of the concentration dependent diffusion coefficient reduces significantly the diffusivity, which affects the cell voltage in a surprisingly non-linear behavior.

Most important, Fig. 11 shows that the concentration dependent diffusion coefficient 114 could explain the decrease of the capacity at the end of discharge, e.g. here at $E = 2.6$V, for increasing discharge current densities (*c.f.* the experimental data in Fig. 1). Wu et al. state in Ref. 2 that "the electrode capacity measured at the end of discharge decreases with increasing rate, as a result of transport limitations in the electrode". This can be confirmed on the basis of concentration dependent diffusion coefficient $D_{\mathrm{A}} = (1 - y_{\mathrm{A}}) \cdot \hat{D}_{\mathrm{A}}$ with $\hat{D}_{\mathrm{A}} = \text{const.}$

BV 4: Finite conductivity in the electrolyte.—First note that an infinite fast diffusion in the electrolyte yet entails $y_{\mathrm{E}} = \bar{y}_{\mathrm{E}}$, whereby the (coupled) transport equation system 23–24 of the electrolyte reduces to

$$i = -\Lambda_{\mathrm{E}} n_{\mathrm{E}} \partial_x \varphi_{\mathrm{E}}, \qquad [117]$$

which yields

$$U_{\mathrm{E}}^{\mathrm{bulk}} = -R_{\mathrm{E}}^{\mathrm{bulk}} \cdot i \quad \text{with} \quad R_{\mathrm{E}}^{\mathrm{bulk}} = \frac{d_{\mathrm{E}}}{\Lambda_{\mathrm{E}} n_{\mathrm{E}}}. \qquad [118]$$

Employing the scaling 71 of the current density i, i.e. $i = i_{\mathrm{A}}^C C_h$ yields

$$U_{\mathrm{E}}^{\mathrm{bulk}} = -\frac{d_{\mathrm{E}}}{\Lambda_{\mathrm{E}} n_{\mathrm{E}}} \cdot i_{\mathrm{A}}^C C_h = \frac{d_{\mathrm{E}}}{d_{\mathrm{A}}} \frac{\sigma_{\mathrm{A}}^C}{\Lambda_{\mathrm{E}} n_{\mathrm{E}}} \frac{k_{\mathrm{B}} T}{e_0} C_h, \qquad [119]$$

which motivates the decomposition

$$\Lambda_{\mathrm{E}} n_{\mathrm{E}}^R = \sigma_{\mathrm{E}}^R = \sigma_{\mathrm{A}}^C \cdot \widetilde{\sigma}_{\mathrm{E}} \quad \text{with} \quad \sigma_{\mathrm{A}}^C = d_{\mathrm{A}} \cdot i_{\mathrm{A}}^C \cdot \frac{e_0}{k_{\mathrm{B}} T} = \frac{d_{\mathrm{A}}^2 q_{\mathrm{A}}^V}{1\,[h]} \cdot \frac{e_0}{k_{\mathrm{B}} T}. \qquad [120]$$

Here n_{E}^R is a constant reference electrolyte concentration, e.g. $1\,\mathrm{mol\,L^{-1}}$, and $\sigma_{\mathrm{E}}^R = \Lambda_{\mathrm{E}} n_{\mathrm{E}}^R$ is the corresponding reference conductivity. Hence

$$U_{\mathrm{E}}^{\mathrm{bulk}} = -\widetilde{d} \cdot \widetilde{c}_{\mathrm{E}}^R \cdot \frac{k_{\mathrm{B}} T}{e_0} \frac{C_h}{\widetilde{\sigma}_{\mathrm{E}}} \quad \text{with} \quad \widetilde{d} := \frac{d_{\mathrm{E}}}{d_{\mathrm{A}}} \quad \text{and} \quad \widetilde{c}_{\mathrm{E}}^R := \left(\frac{n_{\mathrm{E}}^R}{\bar{n}_{\mathrm{E}}}\right), \qquad [121]$$

whereby the cell voltage is

$$E = E_{\mathrm{A,C}} - \frac{k_{\mathrm{B}} T}{e_0} \left(f_{\mathrm{A}}(y_{\mathrm{A}}|_{\mathrm{AE}}(t; i)) - g^{-1}\left(-\frac{C_h}{\widetilde{L}}\right) + \frac{C_h}{\widetilde{\sigma}_{\mathrm{A}}} + \widetilde{d}\, \widetilde{c}_{\mathrm{E}}^R \frac{C_h}{\widetilde{\sigma}_{\mathrm{E}}} \right) \qquad [122]$$

$$= E^{(4)}(Q/Q_{\mathrm{A}}^V; C_h, \widetilde{L}, \widetilde{\sigma}_{\mathrm{A}}, \widetilde{D}_{\mathrm{A}}, \widetilde{\sigma}_{\mathrm{E}}, \widetilde{d}, \widetilde{c}_{\mathrm{E}}^R). \qquad [123]$$

Hence, finite conductivity in the electrolyte linearly decreases the cell voltage and scales also with the ratio of the electrode width to the electrolyte width, i.e. $\widetilde{d}$. The quantity $\widetilde{c}_{\mathrm{E}}^R$ accounts for concentration dependence of the electrolyte conductivity.

Correspondingly we define the electrolyte conductivity overpotential $\eta_{\mathrm{E}}^{\Lambda}$ as

$$\eta_{\mathrm{E}}^{\sigma} := E^{(3)} - E^{(4)} = \frac{k_{\mathrm{B}} T}{e_0} \widetilde{d}\, \widetilde{c}_{\mathrm{E}}^R \frac{C_h}{\widetilde{\sigma}_{\mathrm{E}}}. \qquad [124]$$

BV 5: Finite diffusion in the electrolyte phase.—The final contribution to the surface reaction R is the space dependent electrolyte concentration. We have yet assumed $y_{\mathrm{E}} = \text{const.}$ with respect to space, however, in general the (coupled) equation system 23–24 has to be solved.

Note that $t_{\mathrm{E}_C} = \text{const.}$ simplifies the (coupled) equation system 23–24 to

$$\frac{\partial n_{\mathrm{E}}}{\partial t} = \partial_x \left(D_{\mathrm{E}} \cdot n_{\mathrm{E}}^{\mathrm{tot}}\, \Gamma_{\mathrm{E}}^{\mathrm{tf}} \cdot \partial_x y_{\mathrm{E}} \right) \qquad [125]$$

$$i = -S_{\mathrm{E}} \cdot n_{\mathrm{E}}^{\mathrm{tot}}\, \Gamma^{\mathrm{tf}} \partial_x y_{\mathrm{E}} - \Lambda_{\mathrm{E}} n_{\mathrm{E}} \partial_x \varphi_{\mathrm{E}}. \qquad [126]$$

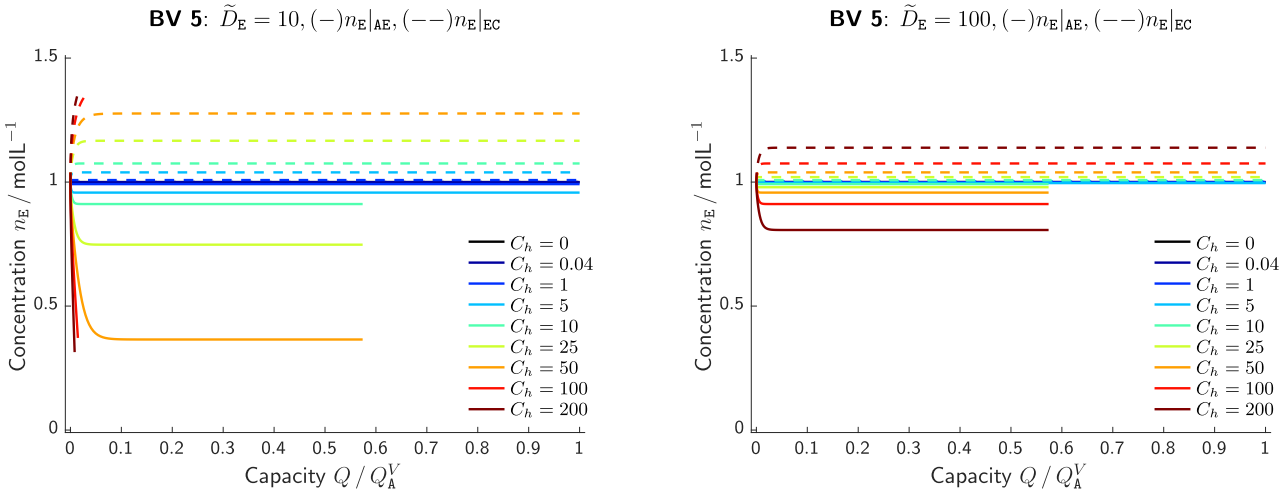

Figure 12. Numerical computation of the cation interface concentrations $n_{\mathrm{E}}|\mathrm{AE}$ and $n_{\mathrm{E}}|\mathrm{EC}$ in the electrolyte for slow ($\widetilde{D}_{\mathrm{E}} = 10$) and fast ($\widetilde{D}_{\mathrm{E}} = 100$) diffusion and various C-rates C_h.

Further, $J_{\mathrm{E}} = -D_{\mathrm{E}} \cdot n_{\mathrm{E}}^{\mathrm{tot}}\, \Gamma_{\mathrm{E}}^{\mathrm{tf}} \cdot \partial_x y_{\mathrm{E}} + \frac{t_{\mathrm{E}C}}{e_0} i$ entails at the interface $\Sigma_{\mathrm{A,E}}$ the condition

$$-D_{\mathrm{E}} \cdot n_{\mathrm{E}}^{\mathrm{tot}}\, \Gamma_{\mathrm{E}}^{\mathrm{tf}} \cdot \partial_x y_{\mathrm{E}}\big|_{\mathrm{AE}} = \frac{1 - t_{\mathrm{E}C}}{e_0} i \qquad [127]$$

We assume that the average electrolyte concentration n_{E} is constant in time, i.e.

$$\frac{\partial \overline{n}_{\mathrm{E}}}{\partial t} = 0 \quad \text{with} \quad \overline{n}_{\mathrm{E}} = \frac{1}{d_{\mathrm{E}}} \int_{x_{\mathrm{EC}}}^{x_{\mathrm{AE}}} n_{\mathrm{E}} dx. \qquad [128]$$

which yields at the right boundary $x = x_{\mathrm{EC}}$ the condition

$$D_{\mathrm{E}} \cdot n_{\mathrm{E}}^{\mathrm{tot}}\, \Gamma_{\mathrm{E}}^{\mathrm{tf}} \cdot \partial_x y_{\mathrm{E}}\big|_{x=x_{\mathrm{EC}}} = \frac{1 - t_{\mathrm{E}C}}{e_0} i. \qquad [129]$$

The concept of an *ideally polarizable* counter-electrode Ω_{C}, positioned at $x = x_{\mathrm{EC}}$, delivers (or consumes) hence exactly the amount of ions in the electrolyte which flow in (or out) of Ω_{E} at $x = x_{\mathrm{AE}}$, with keeping the reaction 45 in thermodynamic equilibrium. The initial value is

$$y_{\mathrm{E}}(x, t = 0) = y_{\mathrm{E}}(\overline{n}_{\mathrm{E}}) \qquad [130]$$

where $\overline{n}_{\mathrm{E}}$ is the prescribed *average* electrolyte concentration.

We introduce the scalings

$$\tau = C_h \frac{t}{[h]} \in [0, 1], \xi = \frac{x}{d_{\mathrm{E}}} \in [0, 1], \frac{n_{\mathrm{E}}^{\mathrm{tot}}(\xi, \tau)}{n_{\mathrm{E}}^{R}} =: \widetilde{c}_{\mathrm{E}}^{\mathrm{tot},R}(\xi, \tau) \qquad [131]$$

$$\Lambda_{\mathrm{E}} n_{\mathrm{E}}^{R} = \widetilde{\sigma}_{\mathrm{E}} \cdot \sigma_{\mathrm{A}}^{C}, i = i_C \cdot C_h, \widetilde{d} = \frac{d_{\mathrm{E}}}{d_{\mathrm{A}}} \qquad [132]$$

with $\sigma_{\mathrm{A}}^{C} = d_{\mathrm{A}} \cdot i_{\mathrm{A}}^{C} \cdot \frac{e_0}{k_{\mathrm{B}} T}$ and $i_{\mathrm{A}}^{C} = \frac{d_{\mathrm{A}} \cdot q_{\mathrm{A}}^{V}}{1[\mathrm{h}]}$. This yields for 125

$$C_h \frac{d_{\mathrm{E}}^2}{1\,[h]} \cdot \frac{1}{D_{\mathrm{E}}} \cdot h_{\mathrm{E}} \cdot \frac{\partial y_{\mathrm{E}}}{\partial \tau} = \partial_{\xi}(\widetilde{c}_{\mathrm{E}}^{\mathrm{tot},R} \Gamma_{\mathrm{E}}^{\mathrm{tf}} \cdot \partial_{\xi} y_{\mathrm{E}}) \quad \text{with} \quad h_{\mathrm{E}} := \frac{1}{n_{\mathrm{E}}^{R}} \frac{\partial n_{\mathrm{E}}}{\partial y_{\mathrm{E}}}. \qquad [133]$$

The corresponding non-dimensional boundary conditions at $\xi = 0$ reads

$$(\widetilde{c}_{\mathrm{E}}^{\mathrm{tot},R} \Gamma_{\mathrm{E}}^{\mathrm{tf}} \partial_{\xi} y_{\mathrm{E}})\big|_{\xi=0} = d_{\mathrm{E}} \frac{1}{n_{\mathrm{E}}^{R}} \frac{1}{D_{\mathrm{E}}} \frac{1 - t_{\mathrm{E}C}}{e_0} \cdot i \qquad [134]$$

which introduces (implicitly) the scaling

$$D_{\mathrm{E}} = \widetilde{D}_{\mathrm{E}} \cdot \left(\frac{q_{\mathrm{A}}^{V}}{e_0 n_{\mathrm{E}}^{R}} (1 - t_{\mathrm{E}C}) \cdot \frac{d_{\mathrm{A}} d_{\mathrm{E}}}{1\,[\mathrm{h}]} \right) \qquad [135]$$

leaving

$$(\widetilde{c}_{\mathrm{E}}^{\mathrm{tot},R} \Gamma_{\mathrm{E}}^{\mathrm{tf}} \partial_{\xi} y_{\mathrm{E}})\big|_{\xi=0} = \frac{C_h}{\widetilde{D}_{\mathrm{E}}} \quad \text{and} \quad (\widetilde{c}_{\mathrm{E}}^{\mathrm{tot},R} \Gamma_{\mathrm{E}}^{\mathrm{tf}} \partial_{\xi} y_{\mathrm{E}})\big|_{\xi=1} = \frac{C_h}{\widetilde{D}_{\mathrm{E}}}. \qquad [136]$$

The balance Equation 125 then reads

$$\widetilde{d} \cdot \widetilde{q}^{V} \cdot \widetilde{t}_{\mathrm{E}} \frac{C_h}{\widetilde{D}_{\mathrm{E}}} h_{\mathrm{E}}(y_{\mathrm{E}}) \frac{\partial y_{\mathrm{E}}}{\partial \tau} = \partial_{\xi}(\widetilde{c}_{\mathrm{E}}^{\mathrm{tot},R} \Gamma_{\mathrm{E}}^{\mathrm{tf}} \cdot \partial_{\xi} y_{\mathrm{E}}) \qquad [137]$$

with

$$\widetilde{q}^{V} := \frac{q_{\mathrm{E}}^{V}}{q_{\mathrm{A}}^{V}}, q_{\mathrm{E}}^{V} = 2 e_0 n_{\mathrm{E}}^{R} \quad \text{and} \quad \widetilde{t}_{\mathrm{E}} = \frac{1}{2 \cdot (1 - t_{\mathrm{E}C})}. \qquad [138]$$

Note that the 2 in q_{E}^{V} accounts for the charge of cations and anions. The charge capacity q_{E}^{V} of a 1mol L^{-1} electrolyte is

$$q_{\mathrm{E}}^{V} = 2 e_0 n_{\mathrm{E}}^{R} \approx 53\,[\mathrm{mA\,h\,cm^{-3}}] \qquad [139]$$

whereby

$$\widetilde{q}^{V} = \frac{45}{1294} = 0.042553. \qquad [140]$$

The dimensionless transference number $\widetilde{t}_{\mathrm{E}} \approx 1$ and $\widetilde{d} = 5$. The PDE is solved with MATLAB's pdepe function, and details are given in the appendix A3. We denote the numerical solution of y_{E} with $\hat{y}_{\mathrm{E}}$ and emphasize that the capacity is yet $Q/Q_{\mathrm{A}}^{V} = \tau$. The numerical solutions $\hat{y}_{\mathrm{E}}$ at the respective boundaries $x = x_{\mathrm{AE}}$ and $x = x_{\mathrm{EC}}$ are

$$y_{\mathrm{E}}\big|_{\mathrm{AE}}^{+} = \hat{y}_{\mathrm{E}}|_{\xi=0} \quad \text{and} \quad y_{\mathrm{E}}\big|_{\mathrm{EC}}^{-} = \hat{y}_{\mathrm{E}}|_{\xi=1}. \qquad [141]$$

We discuss now briefly the concentration distribution in the electrolyte as function of the C-rate C_h and the diffusion coefficient $\widetilde{D}_{\mathrm{E}}$ based on numerical solutions of 125 with boundary conditions 127 and 129.

Fig. 12 displays computations of the electrolytic cation concentration at the interface $\Sigma_{\mathrm{A,E}}$ of the intercalation electrode, i.e. $n_{\mathrm{E}}|_{\mathrm{AE}}$, and at the interface $\Sigma_{\mathrm{E,C}}$ of the counter electrode, i.e. $n_{\mathrm{E}}|_{\mathrm{EC}}$ for slow electrolytic diffusion ($\widetilde{D}_{\mathrm{E}} = 1$, left) and fast diffusion ($\widetilde{D}_{\mathrm{E}} = 10$, right) for various values of the C-rate.

After a short time the concentration yields a stationary state and Fig. 13 displays the stationary concentration $n_{\mathrm{E}}(x)$ in the electrolyte, again for slow and fast diffusion as well as for various C-rates.

Note, however, that the concentration variation of y_{E} has additionally an impact on the voltage drop U_{E}. First reconsider that 126 rewrites as

$$U_{\mathrm{E}} = -\frac{d_{\mathrm{E}}}{\Lambda_{\mathrm{E}} n_{\mathrm{E}}^{R}} \left(\frac{1}{d_{\mathrm{E}}} \int_{x_{\mathrm{EC}}}^{x_{\mathrm{AE}}} \frac{n_{\mathrm{E}}^{R}}{n_{\mathrm{E}}} dx \right) \cdot i + \frac{k_{\mathrm{B}} T}{e_0} (2 t_C - 1) \big(f_{\mathrm{E}}(y_{\mathrm{E}}|_{\mathrm{AE}}) - f_{\mathrm{E}}(y_{\mathrm{E}}|_{\mathrm{EC}}) \big). \qquad [142]$$

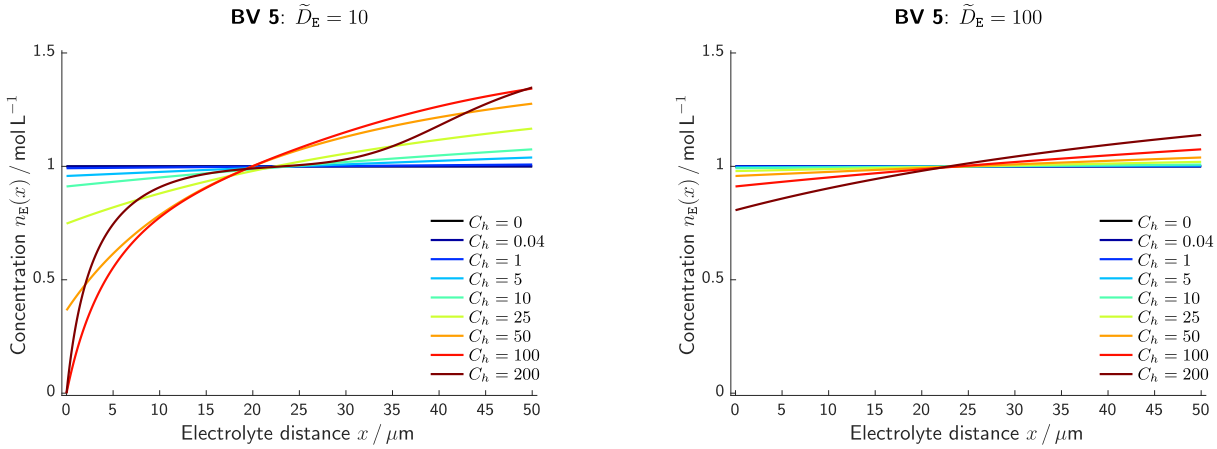

Figure 13. Numerical computation of the stationary cation distribution in the electrolyte for slow ($\widetilde{D}_{\mathrm{E}} = 10$) and fast ($\widetilde{D}_{\mathrm{E}} = 100$) diffusion and various C-rates C_h.

since

$$\frac{S_{\mathrm{E}}}{\Lambda_{\mathrm{E}}} = \frac{k_{\mathrm{B}}T}{e_0}(2t_C - 1). \qquad [143]$$

We abbreviate

$$\bar{c}_{\mathrm{E}}^R := \left(\frac{1}{d_{\mathrm{E}}}\int_{x_{\mathrm{EC}}}^{x_{\mathrm{AE}}} \frac{n_{\mathrm{E}}^R}{n_{\mathrm{E}}} dx\right) \qquad [144]$$

and insert the scaling $\Lambda_{\mathrm{E}} n_{\mathrm{E}}^R = \widetilde{\sigma}_{\mathrm{E}} \cdot \sigma_{\mathrm{A}}^C$ which yields

$$U_{\mathrm{E}} = -\widetilde{d}\bar{c}_{\mathrm{E}}^R \cdot \frac{k_{\mathrm{B}}T}{e_0}\frac{C_h}{\widetilde{\sigma}_{\mathrm{E}}} + \frac{k_{\mathrm{B}}T}{e_0}(2t_C - 1)\big(f_{\mathrm{E}}(y_{\mathrm{E}}|_{\mathrm{AE}}) - f_{\mathrm{E}}(y_{\mathrm{E}}|_{\mathrm{EC}})\big). \qquad [145]$$

The overall cell voltage of **BV 5** is then

$$E = E_{\mathrm{A,C}} - \frac{k_{\mathrm{B}}T}{e_0}\Bigg(f_{\mathrm{A}}(\hat{y}_{\mathrm{A}}|_{\mathrm{AE}}) - 2\cdot t_C\big(f_{\mathrm{E}}(\hat{y}_{\mathrm{E}}|_{\mathrm{AE}}) - f_{\mathrm{E}}(\hat{y}_{\mathrm{E}}|_{\mathrm{EC}})$$
$$-g^{-1}\left(-\frac{C_h}{\widetilde{L}}\right) + \frac{C_h}{\widetilde{\sigma}_{\mathrm{A}}} + \widetilde{d}\,\bar{c}_{\mathrm{E}}^R\frac{C_h}{\widetilde{\sigma}_{\mathrm{E}}}\Bigg) \qquad [146]$$

$$= E^{(5)}(s, C_h; \widetilde{L}, \widetilde{\sigma}_{\mathrm{A}}, \widetilde{D}_{\mathrm{A}}, \widetilde{\sigma}_{\mathrm{E}}, \widetilde{D}_{\mathrm{E}}, t_{\mathrm{E_C}}, \widetilde{d}, \bar{n}_{\mathrm{E}}). \qquad [147]$$

In order to show the impact of the electrolyte concentration variation on the cell voltage E, assume $U_{\mathrm{E}}^{\mathrm{bulk}} = U_{\mathrm{A}}^{\mathrm{bulk}} = 0$ as well infinite fast diffusion in the active particle phase Ω_{A}. This yields

$$E = E_{\mathrm{A,C}} - \frac{k_{\mathrm{B}}T}{e_0}\left(f_{\mathrm{A}}(\bar{y}_{\mathrm{A}}) - 2\cdot t_C\big(f_{\mathrm{E}}(\hat{y}_{\mathrm{E}}|_{\mathrm{AE}}) - f_{\mathrm{E}}(\hat{y}_{\mathrm{E}}|_{\mathrm{EC}}) - g^{-1}\left(-\frac{C_h}{\widetilde{L}}\right)\right) \qquad [148]$$

and numerical computations of the cell voltage for slow and fast diffusion are shown in Fig. 14.

Overpotential.—Due to the (stationary) concentration gradients in the electrolyte (*c.f.* Fig. 13) we have a diffusional overpotential $\eta_{\mathrm{E}}^{\mathrm{D}}$, which can be defined as

$$\eta_{\mathrm{E}}^{\sigma} := E^{(4)} - E^{(5)}$$
$$= \frac{k_{\mathrm{B}}T}{e_0}\left(\widetilde{d}\,(\widetilde{c}_{\mathrm{E}}^R - \bar{c}_{\mathrm{E}}^R)\frac{C_h}{\widetilde{\sigma}_{\mathrm{E}}} - 2\cdot t_C\big(f_{\mathrm{E}}(\hat{y}_{\mathrm{E}}|_{\mathrm{AE}}) - f_{\mathrm{E}}(\hat{y}_{\mathrm{E}}|_{\mathrm{EC}})\right) \qquad [149]$$

$$\approx -\frac{k_{\mathrm{B}}T}{e_0}2\cdot t_C\big(f_{\mathrm{E}}(\hat{y}_{\mathrm{E}}|_{\mathrm{AE}}) - f_{\mathrm{E}}(\hat{y}_{\mathrm{E}}|_{\mathrm{EC}})\big) \qquad [150]$$

Fig. 15 displays numerical computations of the overpotential η_{E}^D for slow and fast diffusion in the electrolyte.

The *recursive* definition of the various overpotentials allows us to write

$$E = E^{(0)}(\bar{y}_{\mathrm{A}}) - \eta^R - \eta_{\mathrm{A}}^D - \eta_{\mathrm{A}}^{\sigma} - \eta_{\mathrm{E}}^D - \eta_{\mathrm{E}}^{\sigma} \qquad [151]$$

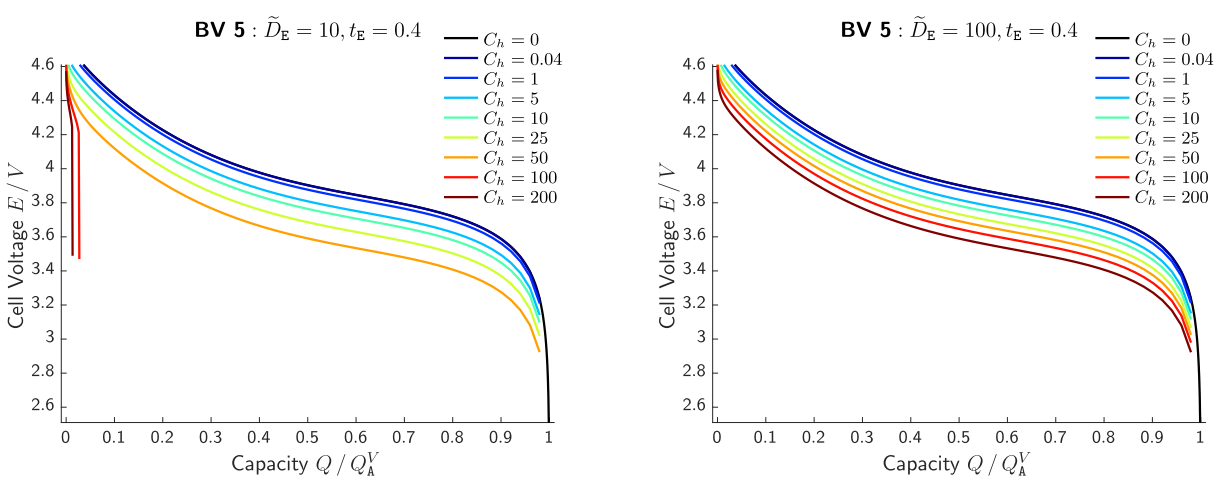

Figure 14. Computed cell voltage according to 148 with numerical solutions shown in Fig. 12 of the interface concentrations $\hat{y}_{\mathrm{E}}|_{\mathrm{AE}}$ and $\hat{y}_{\mathrm{E}}|_{\mathrm{EC}}$ for various discharge rates.

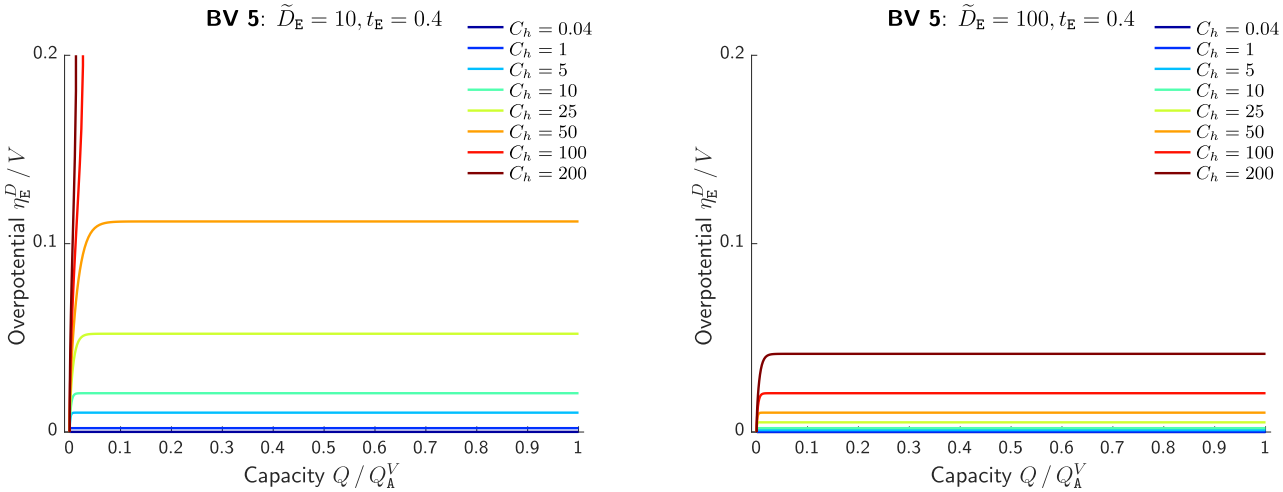

Figure 15. Diffusional overpotential of the electrolyte for slow and fast diffusion computed from numerical solutions of the interface concentrations $\hat{y}_{\mathrm{E}}|_{\mathrm{AE}}|$ and $\hat{y}_{\mathrm{E}}|\mathrm{EC}$ and Eq. 149.

with one overpotential for each non-equilibrium process, measuring the deviation from the equilibrium of the respective process. This decomposition is hence a useful tool to systematically investigate the contribution of each process in broadly conceived experimental or numerical studies of a cell batch with varying parameters.

Internal resistance.—Note that we can also compute the internal resistance R^{int} of the electrochemical cell via the implicit definition

$$E - E^{(0)} = R \cdot I. \qquad [152]$$

With $I = \frac{i_{\mathrm{A}}^C \cdot C_h}{A}$ we obtain for the specific resistance

$$R = \frac{E - E^{(0)}}{I} = -\frac{A}{i_{\mathrm{A}}^C} \frac{(\eta^R + \eta_{\mathrm{A}}^D + \eta_{\mathrm{A}}^\sigma + \eta_{\mathrm{E}}^D + \eta_{\mathrm{A}}^\sigma)}{C_h}$$
$$= R_{\mathrm{A}} \cdot (r^R + r_{\mathrm{A}}^D + r_{\mathrm{A}}^\Sigma + r_{\mathrm{E}}^D + r_{\mathrm{E}}^\sigma) \qquad [153]$$

with

$$R_{\mathrm{A}} = \frac{k_{\mathrm{B}} T}{e_0} \frac{A}{i_{\mathrm{A}}^C} \qquad [154]$$

and

- intercalation reaction resistance

$$r^R = -g^{-1}\left(-\frac{C_h}{\widetilde{L}}\right) \frac{1}{C_h} \overset{\text{Tafel}}{\approx} \frac{1}{\widetilde{L}}, \qquad [155]$$

- active phase diffusional resistance

$$r_{\mathrm{A}}^D = \left(f_{\mathrm{A}}(\bar{y}_{\mathrm{A}}) - f_{\mathrm{A}}(\hat{y}_{\mathrm{A}}|_{\mathrm{AE}})\right) \frac{1}{C_h}, \qquad [156]$$

- active phase conduction resistance

$$r_{\mathrm{A}}^\sigma = \frac{1}{\widetilde{\sigma}_{\mathrm{A}}}, \qquad [157]$$

- electrolyte diffusional resistance

$$r_{\mathrm{E}}^D = 2 \cdot t_C \left(f_{\mathrm{E}}(\hat{y}_{\mathrm{E}}|_{\mathrm{AE}}) - f_{\mathrm{E}}(\hat{y}_{\mathrm{E}}|_{\mathrm{EC}})\right) \cdot \frac{1}{C_h}, \qquad [158]$$

- electrolyte conduction resistance

$$r_{\mathrm{E}}^\sigma = \frac{1}{\widetilde{\sigma}_{\mathrm{E}}}. \qquad [159]$$

Conclusions

Validation.—Equation 146 for the general relation for the cell voltage E in a simple, non-porous intercalation electrode. Note, however, that the scalings, discussion and parameter study of Discussion section can be straight forward adapted to porous electrodes.

We provide finally a validation study for NMC with the following set of the non-dimensional parameters

$$\widetilde{L} = 1, \widetilde{D}_{\mathrm{A}} = 10, \widetilde{\sigma}_{\mathrm{A}} = 100, \widetilde{D}_{\mathrm{E}} = 100, \widetilde{\sigma}_{\mathrm{E}} = 100 \qquad [160]$$

and a concentration dependent diffusion coefficient $D_{\mathrm{A}} = (1 - y_{\mathrm{A}})\hat{D}_{\mathrm{A}}$. In absolute values, these translate to:

- exchange current density $i_0 = \widetilde{L} \cdot i_{\mathrm{A}}^C = 1.2597 \left[m\mathrm{Acm}^{-2}\right]$,
- NMC electric conductivity of $\sigma_{\mathrm{A}} = \widetilde{\sigma}_{\mathrm{A}} \cdot \frac{d_{\mathrm{A}}^2 q_{\mathrm{A}}^V}{1[h]} \cdot \frac{e_0}{k_{\mathrm{B}} T} = 4.9014 \left[m\mathrm{Scm}^{-1}\right]$,
- lithium diffusion coefficient in NMC $\hat{D}_{\mathrm{A}} = \widetilde{D}_{\mathrm{A}} \cdot \frac{d_{\mathrm{A}}^2}{1[\mathrm{h}]} = 2.7778 \cdot 10^{-10} \left[\mathrm{cm}^2\,\mathrm{s}^{-1}\right]$,
- electrolyte conductivity $\sigma_{\mathrm{E}} = \widetilde{\sigma}_{\mathrm{E}} \cdot \frac{d_{\mathrm{A}}^2 q_{\mathrm{A}}^V}{1[h]} \cdot \frac{e_0}{k_{\mathrm{B}} T} = 4.9014 \left[m\mathrm{Scm}^{-1}\right]$,
- electrolyte diffusion coefficient $\hat{D}_{\mathrm{E}} = \widetilde{D}_{\mathrm{E}} \cdot \left(\frac{q_{\mathrm{A}}^V}{e_0 n_{\mathrm{E}}^R}(1 - t_{\mathrm{E}_C}) \cdot \frac{d_{\mathrm{A}} d_{\mathrm{E}}}{1[\mathrm{h}]}\right) = 1.9583 \cdot 10^{-6} \left[\mathrm{cm}^2\,\mathrm{s}^{-1}\right]$

Figure 16 displays the numerical computation of the cell voltage. In comparison to experimental data for a cell of the same dimension (however, neglecting porosity), we obtain a good qualitative and quantitative agreement to Fig. 1.

This is especially remarkable since we assumed essentially for all non-equilibrium parameters constant values, i.e. no concentration dependence of the diffusion coefficient D_{E}, the cation transference number t_{E}, and the conductivities. In particular we assumed that the exchange current density $e_0 \underset{s}{L}$ is also constant, yielding the reasonable results of the last section. Note, however, that it is frequently assumed that the exchange current density is dependent on cation concentration at the interface $\Sigma_{\mathrm{A,E}}$. We discuss this aspect in the next section and emphasize again that a consistent thermodynamic modeling as well as coupling through the surface reaction rate yields the reasonable results of the last sections. The scaling of all non-equilibrium parameters to the C-rate is quite illustrative for the sake of galvanostatic discharge and especially for the systematic *search* of the parameters of a specific battery.

Discussion of the exchange current density.—The preceding discussion of the cell voltage E was based on the model 38 of the surface

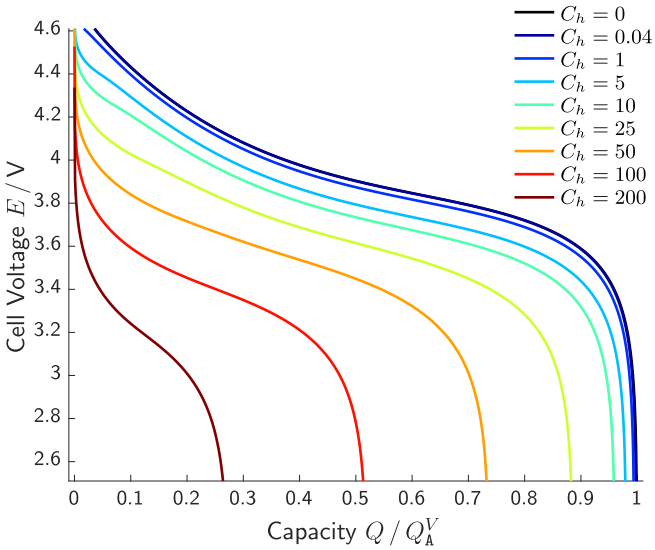

Figure 16. Computed cell voltage E as function of the capacity Q/Q_A^V with parameters of the non-equilibrium processes according to 160.

reaction rate $\underset{s}{R}$, i.e.

$$\underset{s}{R} = \underset{s}{L} \cdot \left(e^{\alpha \cdot \frac{1}{k_B T} \underset{s}{\lambda}} - e^{-(1-\alpha) \cdot \frac{1}{k_B T} \underset{s}{\lambda}} \right) \quad \text{with}$$
$$\underset{s}{\lambda} = \underset{s}{\mu}_{A_C} + \kappa_E \cdot \underset{s}{\mu}_{E_S} - \underset{s}{\mu}_{E_C} - \underset{s}{\mu}_{A_e}, \qquad [161]$$

with $\underset{s}{L} = \text{const.}$ In Discussion of the model parameters section we showed that double layer charging effects are negligible under galvanostatic conditions, whereby the measurable current density i is directly related to $e_0 \underset{s}{R}$, i.e. $i = e_0 \underset{s}{R}$. The surface affinity $\underset{s}{\lambda}$ is related to the cell voltage E via 48, i.e.

$$\underset{s}{\lambda} = e_0(E + U_A^{\text{bulk}} - U_E^{\text{bulk}} - E_{A,C}) + k_B T \left(f_A - f_E|_{AE} + f_E|_{EC} \right) \quad [162]$$

with

$$f_E(y_E) := \ln \left(\frac{y_E}{\left(\hat{y}_{E_S}(y_E)\right)^{\kappa_E}} \right) \quad , \qquad [163]$$

$$f_A(y_A) := \ln \left(\frac{\frac{1}{\omega_A} y_A}{1 + \frac{1-\omega_A}{\omega_A} y_A} \right) - \omega_A \cdot \ln \left(\frac{1 - y_A}{1 + \frac{1-\omega_A}{\omega_A} y_A} \right) + \gamma_A \cdot h_A(y_A). \qquad [164]$$

Note that we have introduce the open circuit potential $E^{(0)}$ in BV 0: Open circuit potential section as

$$E^{(0)}(\bar{y}_A) = E_{A,C} - \frac{k_B T}{e_0} f_A(\bar{y}_A). \qquad [165]$$

We can also evaluate the open circuit potential function $E^{(0)}$ with the interface concentration $y_A|_{AE}$, i.e.

$$E^{(0)}(y_{AE}) = E_{A,C} - \frac{k_B T}{e_0} f_A(y_{AE}). \qquad [166]$$

Note that this is a crucially different to 165 when finite diffusion in the active particle phase is considered, see BV 1: Infinite fast diffusion and conductivity in the active particle and the electrolyte section. However, this allows us rewrite the surface affinity $\underset{s}{\lambda}$ as

$$\underset{s}{\lambda} = e_0(\varphi_A - \varphi_E - E^{(0)}(y_A|_{AE})) - k_B T \, f_E|_{AE} \qquad [167]$$
$$= e_0(\varphi_A - \widetilde{\varphi}_E - E^{(0)}(y_A|_{AE})) = e_0(\widetilde{\eta}_{AE} - E^{(0)}(y_A|_{AE})) \qquad [168]$$

with

$$\varphi_A = \varphi|_{AE}^{-}, \; \varphi_E = \varphi|_{AE}^{+}, \; \widetilde{\varphi}_E := \varphi|_{AE}^{+} + \frac{k_B T}{e_0} f_E(y_E|_{AE}) \qquad [169]$$

and

$$\eta_{AE} := \varphi_A - \widetilde{\varphi}_E = U_{AE}^{DL} - \frac{k_B T}{e_0} f_E|_{AE}. \qquad [170]$$

This yields

$$i = e_0 \underset{s}{L} \cdot \left(e^{\alpha \cdot \frac{e_0}{k_B T} \left(\widetilde{\eta}_{AE} - E^{(0)}(y_A|_{AE}) \right)} - e^{-(1-\alpha) \frac{e_0}{k_B T} \left(\widetilde{\eta}_{AE} - E^{(0)}(y_A|_{AE}) \right)} \right). \qquad [171]$$

This is the general, thermodynamic consistent version of the Butler–Volmer equation.[4,26] The specific form 171 of the current density i in terms of the *surface overpotential*[1] η_{AE}, the open circuit potential $E^{(0)}(y_A|_{AE})$, and the exchange current density $e_0 \underset{s}{L}$ is widely employed in the literature[28,40] and thus feasible to discuss various material models of $\underset{s}{L}$.

In Refs. 1,41,42 as well as subsequent work we find

$$i^{BV} = i_0^{BV} \cdot \left(e^{\alpha \cdot \frac{e_0}{k_B T} (\eta - E^{(0)}(\bar{y}_A))} - e^{-(1-\alpha) \cdot \frac{e_0}{k_B T} (\eta - E^{(0)}(\bar{y}_A))} \right) \qquad [172]$$

with $\eta = \Phi_1 - \Phi_2$, where Φ_2 "is measured with a lithium reference electrode",[1] p.1527 and Φ_1 the electrostatic potential in the active phase. For the exchange current density i_0^{BV} we find various models:

- In Ref. 41 we find

$$i_0^{BV} = k \cdot (1 - y_A|_{AE})^{(1-\alpha)} (y_A|_{AE})^{\alpha} \quad \text{with} \quad k = \text{const.} \qquad [173]$$

- In Ref. 41 we find

$$i_0^{BV} = k \cdot (1 - y_A|_{AE})^{(1-\alpha)} (y_A|_{AE})^{\alpha} (1 - y_E|_{AE})^{(1-\alpha)} (y_E|_{AE})^{\alpha} \quad \text{with}$$
$$k = \text{const.} \qquad [174]$$

- In Refs. 35,43 we find

$$i_0^{BV} = k \cdot (1 - y_A|_{AE})^{(1-\alpha)} (y_A|_{AE})^{(\alpha)} (y_E|_{AE})^{\alpha} \quad \text{with} \quad k = \text{const.} \qquad [175]$$

This model for the Butler–Volmer-reaction rate became a standard in the literature of modeling intercalation batteries[44–48] and is implemented in various software packaged to simulate battery cycles (i.e. COMSOL, Battery Design Studio,[49] BEST[35,43]) as well as a basis for the interpretation of experimental data.[50]

We compare the Butler–Volmer Equation 172 to the surface reaction rate 171 and discuss the thermodynamic consistency of the three models 173–175 for the exchange current density. Latz et al.,[51] Bazant,[21] and Dreyer et al.[26] also point out the importance of thermodynamic consistency of the Butler–Volmer equation to achieve some overall predictive model since it couples the different thermodynamic bulk models. Dreyer et al.[26] use the same structure 38 of the reaction rate, in combination with a constant exchange current density, however do not study intercalation electrodes.

First of all we mention again that the Butler–Volmer Equation 171 is derived from surface thermodynamics (see Reaction rate based on surface thermodynamics section) and that the exchange current density $e_0 \underset{s}{L}$ is the Onsager coefficient of the surface reaction Onsager coefficient of the intercalation reaction. This yields some necessary constraints on $\underset{s}{L}$ in terms of the functional dependency on the concentrations (or mole fractions) evaluated at the interface $\Sigma_{A,E}$, which are discussed in Onsager coefficient of the intercalation reaction.

By comparison of Eqs. 171 and 172 we obtain

$$\Phi_1 = \varphi|_{AE}^{-} \quad \text{and} \quad \Phi_2 = \varphi|_{AE}^{+} + \frac{k_B T}{e_0} f_E(y_E|_{AE}). \qquad [176]$$

For a metallic lithium counter electrode, where the reaction

$$\text{Li}^+\big|_C + \kappa_E \cdot \text{S}\big|_E \rightleftharpoons \text{Li}^+\big|_E \qquad [177]$$

is in thermodynamic equilibrium we have 45 entails

$$\varphi|^{-}_{x=x_{\mathrm{EC}}} = \varphi|^{+}_{x=x_{\mathrm{EC}}} \frac{1}{e_0}(\mu_{\mathrm{C}_C} - g^R_{\mathrm{A}_C} - \kappa_{\mathrm{E}} g^R_{\mathrm{E}_S}) - \frac{k_{\mathrm{B}}T}{e_0} f_{\mathrm{E}}(y_{\mathrm{E}_C}|_{\mathrm{EC}}) \quad [178]$$

which somehow justifies the interpretation of Φ_2 as the potential "is measured with a lithium reference electrode",[1] p.1527. However, from a thermodynamic point of view this *re-definition* of the potential is not necessary and could lead to inconsistencies when not applied in all balance equations (e.g. of the electrolyte transport) and boundary conditions of the intercalation battery model.

For the exchange current density $e_0 \underset{s}{L}$ we showed in Onsager coefficient of the intercalation reaction section that if $\underset{s}{L}$ is dependent on the concentrations at the interface $\Sigma_{\mathrm{A,E}}$, the dependency for the electrolyte species is necessarily

$$\underset{s}{L} = \underset{s}{L}_{\mathrm{E}}\left(\mu_{\mathrm{E}_C}(y_{\mathrm{E}_C}|^{+}_{\mathrm{AE}}) - e_0 U^{\mathrm{SCL}}_{\mathrm{E}}\right) = \underset{s}{\hat{L}}_{\mathrm{E}}\left(y_{\mathrm{E}_C}|^{+}_{\mathrm{AE}} \cdot \mathrm{e}^{-\frac{e_0}{k_{\mathrm{B}}T} U^{\mathrm{SCL}}_{\mathrm{E}}}\right). \quad [179]$$

and for the intercalated ions in the active phase

$$\underset{s}{L} = \underset{s}{L}_{\mathrm{A}}\left(\mu_{\mathrm{A}_C}(y_{\mathrm{A}_C}|_{\mathrm{AE}})\right) = \underset{s}{\hat{L}}_{\mathrm{A}}(y_{\mathrm{A}_C}|_{\mathrm{AE}}), \quad [180]$$

or overall

$$\underset{s}{L} = \underset{s}{\hat{L}}\left(y_{\mathrm{E}_C}|^{+}_{\mathrm{AE}} \cdot \mathrm{e}^{-\frac{e_0}{k_{\mathrm{B}}T} U^{\mathrm{SCL}}_{\mathrm{E}}}, y_{\mathrm{A}_C}|_{\mathrm{AE}}\right). \quad [181]$$

with $U^{\mathrm{DL}}_{\mathrm{AE}} = \varphi|^{-}_{\mathrm{AE}} - \varphi|^{+}_{\mathrm{AE}}$. Comparing these constraints with the models of the exchange current densities 173–175 clearly shows that the dependency of i^{BV}_0 on the mole fraction $y_{\mathrm{E}_C}|^{+}_{\mathrm{AE}}$ (or concentration $n_{\mathrm{E}_C}|^{+}_{\mathrm{AE}}$) of the electrolyte concentration is not compatible with a reaction rate based on non-equilibrium surface thermodynamics. The concentration dependence is already embedded in the term $f_{\mathrm{E}}(y_{\mathrm{E}_C}|_{\mathrm{AE}})$ of the surface affinity $\underset{s}{\lambda}$ 167. A dependency of the exchange current density on $y_{\mathrm{A}}|_{\mathrm{AE}}$ is in principle compatible with surface thermodynamics. All three models propose

$$i^{\mathrm{BV}}_0 \propto (1 - y_{\mathrm{A}}|_{\mathrm{AE}})^{(1-\alpha)}(y_{\mathrm{A}}|_{\mathrm{AE}})^{\alpha} \quad [182]$$

which in terms of the surface Onsager coefficient would be

$$\underset{s}{L}_{\mathrm{A}} = \underset{s}{L} \cdot 2 \cdot (1 - y_{\mathrm{A}}|_{\mathrm{AE}})^{(1-\alpha)}(y_{\mathrm{A}}|_{\mathrm{AE}})^{\alpha} \quad \text{and} \quad \underset{s}{L} = \text{const.} > 0. \quad [183]$$

In order to discuss the validity, predictability and finally the necessity (or non-necessity) of a concentration dependent surface Onsager coefficient $\underset{s}{L}_{\mathrm{A}}$ (or exchange current density), we pursue the same strategy and scalings as in Discussion section, however, now with the model 183. We compute the cell voltage E as function of the capacity Q/Q^V_{A} and the C-rate C_h in the hierarchy of approximations **BV 1 – BV 5** and compare it to the computations based on the constant Onsager coefficient.

Eq. 51 reduces with negligible double layer contributions to

$$i = -e_0 \underset{s}{L} \cdot 2 \cdot (1 - y_{\mathrm{A}}|_{\mathrm{AE}})^{(1-\alpha)}(y_{\mathrm{A}}|_{\mathrm{AE}})^{\alpha} \cdot g\left(\frac{1}{k_{\mathrm{B}}T}\underset{s}{\lambda}\right). \quad [184]$$

We consider again the scaling

$$e_0 \underset{s}{L} = \widetilde{L} \cdot i^C_{\mathrm{A}} = \widetilde{L}\frac{d_{\mathrm{A}} \cdot q^V_{\mathrm{A}}}{1\,[\mathrm{h}]}. \quad [185]$$

which yields the cell voltage

$$E = E_{\mathrm{A,C}} - \frac{k_{\mathrm{B}}T}{e_0}\left(f_{\mathrm{A}} - f_{\mathrm{E}}|_{\mathrm{AE}} + f_{\mathrm{E}}|_{\mathrm{EC}}\right) - g^{-1}\left(-\frac{\frac{C_h}{L}}{2 \cdot (1 - y_{\mathrm{A}}|_{\mathrm{AE}})^{(1-\alpha)}(y_{\mathrm{A}}|_{\mathrm{AE}})^{\alpha}}\right) - U^{\mathrm{bulk}}_{\mathrm{A}} + U^{\mathrm{bulk}}_{\mathrm{E}}. \quad [186]$$

Consider the approximation of infinite conductivity in both phases as well as infinite fast diffusion in the electrolyte, i.e. the approximation **BV 3**. Fig. 17 shows computations of cell voltage with constant exchange current density as well as concentration dependent exchange current density, for slow ($\widetilde{D}_{\mathrm{A}} = 1$) and fast ($\widetilde{D}_{\mathrm{A}}10$) diffusion in the active particle phase.

The impact of the model 183 for the Onsager coefficient (or the exchange current density) on the cell voltage is surprisingly small. Quite similar to the assumed concentration independence of the diffusion coefficients D_{A} and D_{E} we can conclude that $\underset{s}{L} = \text{const.}$ is a rather good approximation for the overall modeling procedure. However, well defined and reproduce experimental data sets to compute absolute and relative model errors are rare throughout the literature and the deviations in 17 within the experimental variability. We conclude hence that the model 183 is in principle thermodynamically consistent, when embedded rigorously as stated in Modeling section, however, a constant exchange current density produces also very reasonable results and is thus the first choice.

Summary.—In this work we discuss the cell voltage E of a non-porous intercalation half-cell during galvanostatic discharge with a continuum model for the active intercalation phase, the adjacent electrolyte, and boundary conditions coupling the phases. Based on non-equilibrium surface thermodynamics a reaction rate for the intercalation reaction $\mathrm{Li}^+ + \mathrm{e}^- \rightleftharpoons \mathrm{Li}$ is stated and the measured cell voltage E subsequently derived. We emphasize some necessary restrictions on

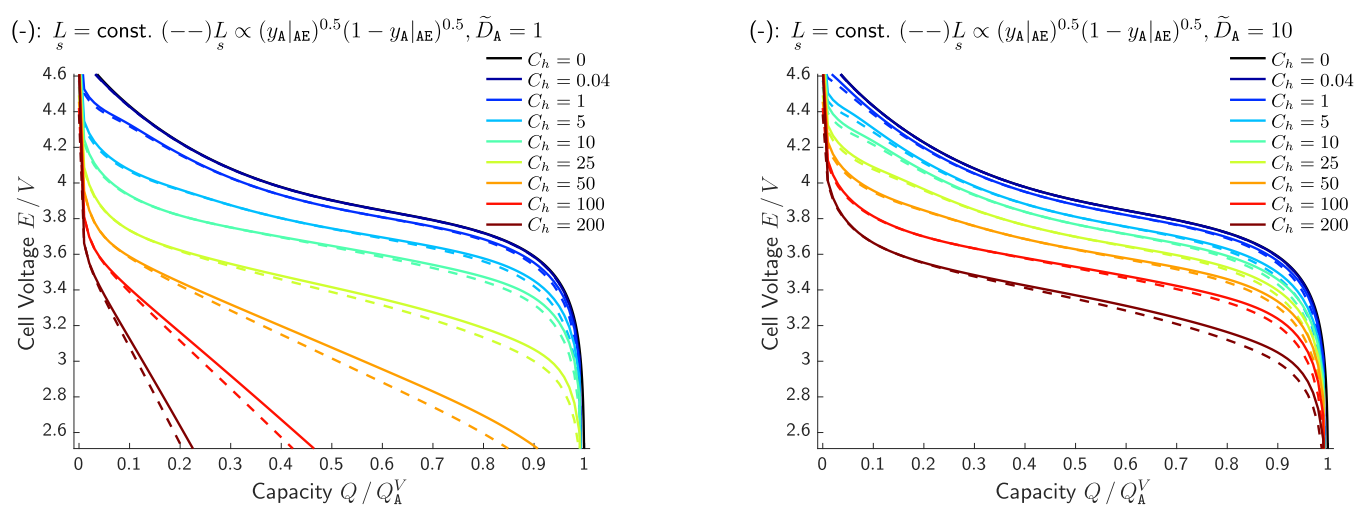

Figure 17. Comparison of the compute cell voltage for the exchange current density according to Eq. 183 (–) and a constant surface Onsager coefficient $\underset{s}{L} = \text{const.}$ for various C-rates and slow diffusion (left) as well as fast diffusion (right).

the exchange current density of the surface reaction rate in terms of concentration dependence to ensure surface thermodynamic consistency.

For the detailed investigation of the non-equilibrium processes, scalings of all non-equilibrium parameters, i.e. the diffusion coefficients D_{A} and D_{E} of the active phase and the electrolyte, conductivity σ_{A} and σ_{E} of both phases, and the exchange current density $e_0 \underset{s}{L}$ of the intercalation reaction, with respect to the 1-C current density i_{A}^C are introduced. The current density i, entering the model via the boundary conditions, is then expressed as multiple of i_{A}^C, i.e. $i = C_h \cdot i$, where C_h is the C-rate. Further we derive an expression for the capacity Q of the intercalation cell, which allows us to compute numerically the cell voltage E as function of the capacity Q for various C-rates C_h. Within a hierarchy of approximations, e.g. open circuit potential, infinite conductivity, infinite fast diffusion, and so forth, we provide simulations of $E = E(C_h, Q)$ for various values of the (non-dimensional) parameters $(\widetilde{\sigma}_{\mathrm{A}}, \widetilde{\sigma}_{\mathrm{E}}, \widetilde{D}_{\mathrm{A}}, \widetilde{D}_{\mathrm{E}}, \widetilde{L})$, scaled with respect to the material constant i_{A}^C. This provides an overall view of the processes and scalings within a lithium ion half cell which is validated at experimental data of $\mathrm{Li}_x\mathrm{Ni}_{1/3}\mathrm{Mn}_{1/3}\mathrm{Co}_{1/3}\mathrm{O}_2$(NMC).

Acknowledgments

The author acknowledges the financial support by the Federal Ministry of Education and Research of Germany (BMBF) in the framework mathematics for innovation (project number 05M18BCA). The author thanks the reviewers for their beneficial remarks.

Appendix A: Electrolyte

Mole fractions.—We consider complete dissociation of the electrolyte and can thus express the mole fractions y_α in terms of n_{E}, i.e.

$$y_{\mathrm{E}_C} = \frac{n_{\mathrm{E}_C}}{n} = \frac{n_{\mathrm{E}}}{n_{\mathrm{E}_S}^R + \left(2 - \frac{(\nu_{\mathrm{E}_A} + \nu_{\mathrm{E}_C})}{\nu_{\mathrm{E}_S}}\right) n_{\mathrm{E}}} \tag{A1}$$

$$y_{\mathrm{E}_S} = \frac{n_{\mathrm{E}_S}}{n} = \frac{n_{\mathrm{E}_S}^R - \frac{(\nu_{\mathrm{E}_A} + \nu_{\mathrm{E}_C})}{\nu_{\mathrm{E}_S}} n_{\mathrm{E}}}{n_{\mathrm{E}_S}^R + \left(2 - \frac{(\nu_{\mathrm{E}_A} + \nu_{\mathrm{E}_C})}{\nu_{\mathrm{E}_S}}\right) n_{\mathrm{E}}}, \tag{A2}$$

and $y_{\mathrm{E}_A} = y_{\mathrm{E}_C}$ according to the electroneutrality condition. Note we assume

$$\nu_{\mathrm{E}_A}^R = \nu_{\mathrm{E}_C}^R = \kappa_{\mathrm{E}} \nu_{\mathrm{E}_S}^R \tag{A3}$$

whereby

$$y_{\mathrm{E}_C} = \frac{n_{\mathrm{E}_C}}{n} = \frac{n_{\mathrm{E}}}{n_{\mathrm{E}_S}^R + 2\left(1 - \kappa_{\mathrm{E}}\right) n_{\mathrm{E}}} \tag{A4}$$

$$y_{\mathrm{E}_S} = \frac{n_{\mathrm{E}_S}}{n} = \frac{n_{\mathrm{E}_S}^R - 2\kappa_{\mathrm{E}} n_{\mathrm{E}}}{n_{\mathrm{E}_S}^R + 2\left(1 - \kappa_{\mathrm{E}}\right) n_{\mathrm{E}}}. \tag{A5}$$

We can also express y_α as function of of n_{E}, i.e.

$$y_{\mathrm{E}_C} = \frac{n_{\mathrm{E}}}{n_{\mathrm{E}}^{\mathrm{tot}}} = \frac{n_{\mathrm{E}}}{n_{\mathrm{E}_S}^R - 2\kappa_{\mathrm{E}} n_{\mathrm{E}}} \tag{A6}$$

Thermodynamic factor.—

$$\Gamma_{\mathrm{E}}^{\mathrm{tf}} = \frac{y_{\mathrm{E}_C}}{k_{\mathrm{B}} T} \frac{\partial \hat{\mu}_{\mathrm{E}_C}}{\partial y_{\mathrm{E}_C}} = 1 + 2\kappa_{\mathrm{E}} \frac{y_{\mathrm{E}}}{1 - 2y_{\mathrm{E}_C}} = \Gamma_{\mathrm{E}}^{\mathrm{tf}}(y_{\mathrm{E}}). \tag{A7}$$

Further

$$n_{\mathrm{E}_C} = y_{\mathrm{E}_C} \cdot n = n_{\mathrm{E}_S}^R \frac{y_{\mathrm{E}_C}}{1 + 2(\kappa_{\mathrm{E}} - 1) y_{\mathrm{E}}} = n_{\mathrm{E}_C}(y_{\mathrm{E}}). \tag{A8}$$

whereby

$$\frac{\partial n_{\mathrm{E}}}{\partial y_{\mathrm{E}}} = n_{\mathrm{E}_S}^R \frac{1 + 2(\kappa_{\mathrm{E}} - 1) y_{\mathrm{E}} - y_{\mathrm{E}} 2(\kappa_{\mathrm{E}} - 1)}{(1 + 2(\kappa_{\mathrm{E}} - 1) y_{\mathrm{E}})^2} = n_{\mathrm{E}_S}^R \frac{1}{(1 + 2(\kappa_{\mathrm{E}} - 1) y_{\mathrm{E}})^2} \tag{A9}$$

and thus

$$h_{\mathrm{E}}(y_{\mathrm{E}}) = \frac{1}{n_{\mathrm{E}}^R} \frac{\partial n_{\mathrm{E}}}{\partial y_{\mathrm{E}}} = \frac{n_{\mathrm{E}_S}^R}{n_{\mathrm{E}}^R} \frac{1}{(1 + 2(\kappa_{\mathrm{E}} - 1) y_{\mathrm{E}})^2} =: . \tag{A10}$$

Finally we have also

$$\widetilde{c}_{\mathrm{E}}^{\mathrm{tot},R}(y_{\mathrm{E}}) = \frac{n_{\mathrm{E}}^{\mathrm{tot}}}{n_{\mathrm{E}}^R} = \frac{n_{\mathrm{E}_S}^R}{n_{\mathrm{E}}^R} \cdot \frac{1}{1 + 2(\kappa_{\mathrm{E}} - 1) y_{\mathrm{E}}} \tag{A11}$$

PDEPE syntax for the electrolyte phase.—We want to solve numerically the problem

$$\widetilde{d} \cdot \widetilde{q}^{\mathrm{V}} \cdot \widetilde{t}_{\mathrm{E}} \frac{C_h}{\widetilde{D}_{\mathrm{E}}} h_{\mathrm{E}}(y_{\mathrm{E}}) \frac{\partial y_{\mathrm{E}}}{\partial \tau} = \partial_\xi (\widetilde{c}_{\mathrm{E}}^{\mathrm{tot}}(y_{\mathrm{E}}) \Gamma_{\mathrm{E}}^{\mathrm{tf}}(y_{\mathrm{E}}) \cdot \partial_\xi y_{\mathrm{E}}) \tag{A12}$$

with boundary conditions

$$(\widetilde{c}_{\mathrm{E}}^{\mathrm{tot},R} \Gamma_{\mathrm{E}}^{\mathrm{tf}} \partial_\xi y_{\mathrm{E}})\big|_{\xi=0} = \frac{C_h}{\widetilde{D}_{\mathrm{E}}} \quad \text{and} \quad \widetilde{(c}_{\mathrm{E}}^{\mathrm{tot},R} \Gamma_{\mathrm{E}}^{\mathrm{tf}} \partial_\xi y_{\mathrm{E}})\big|_{\xi=1} = \frac{C_h}{\widetilde{D}_{\mathrm{E}}} \tag{A13}$$

and

$$h_{\mathrm{E}}(y_{\mathrm{E}}) = \frac{n_{\mathrm{E}_S}^R}{n_{\mathrm{E}}^R} \frac{1}{(1 + 2(\kappa_{\mathrm{E}} - 1) y_{\mathrm{E}})^2} \tag{A14}$$

$$\Gamma_{\mathrm{E}}^{\mathrm{tf}}(y_{\mathrm{E}}) = 1 + 2\kappa_{\mathrm{E}} \frac{y_{\mathrm{E}}}{1 - 2y_{\mathrm{E}_C}} \tag{A15}$$

$$\widetilde{c}_{\mathrm{E}}^{\mathrm{tot},R} = \frac{n_{\mathrm{E}_S}^R}{n_{\mathrm{E}}^R} \frac{1}{1 + 2(\kappa_{\mathrm{E}} - 1) y_{\mathrm{E}}} \tag{A16}$$

Note that it is ever convenient for the numerical computation of $y_{\mathrm{E}} \in (0, 0.5)$ to introduce the variable

$$u = \frac{1}{a} \ln\left(\frac{2y_{\mathrm{E}}}{1 - 2y_{\mathrm{E}}}\right) = \hat{u}(2y_{\mathrm{E}}) \tag{A17}$$

which yields

$$y_{\mathrm{E}} = \frac{1}{2} \cdot \frac{\mathrm{e}^{au}}{1 + \mathrm{e}^{au}} = \frac{1}{2} \hat{y}(u). \tag{A18}$$

The parameter a can be adjusted for numerical computations.

Correspondingly, we obtain

$$h_{\mathrm{E}}(y_{\mathrm{E}}) = h_{\mathrm{E}}(\frac{1}{2} \hat{y}(u)) \tag{A19}$$

$$\Gamma_{\mathrm{E}}^{\mathrm{tf}}(y_{\mathrm{E}}) = \Gamma_{\mathrm{E}}^{\mathrm{tf}}(\frac{1}{2} \hat{y}(u)) \tag{A20}$$

$$\widetilde{c}_{\mathrm{E}}^{\mathrm{tot},R}(y_{\mathrm{E}}) = \widetilde{c}_{\mathrm{E}}^{\mathrm{tot},R}(\frac{1}{2} \hat{y}(u)) \tag{A21}$$

and

$$\partial_\tau y_{\mathrm{E}} = \frac{1}{2} \partial_u \hat{y} \cdot \partial_\tau u, \; \partial_x y_{\mathrm{E}} = \frac{1}{2} \partial_u \hat{y} \cdot \partial_x u \tag{A22}$$

with

$$\partial_u \hat{y} = \frac{a\mathrm{e}^{au}\,(1 + \mathrm{e}^u) - a\mathrm{e}^u\,\mathrm{e}^u}{(1 + \mathrm{e}^{au})^2} = a \frac{\mathrm{e}^{au}}{(1 + \mathrm{e}^{au})^2} =: g_u(u) \tag{A23}$$

This yields

$$\widetilde{p} \cdot \frac{C_h}{\widetilde{D}_{\mathrm{E}}} h_{\mathrm{E}}\left(\frac{1}{2} \hat{y}(u)\right) \frac{1}{2} g_u(u) \frac{\partial u}{\partial \tau} = \partial_\xi \left(\widetilde{c}_{\mathrm{E}}^{\mathrm{tot},R}\left(\frac{1}{2} \hat{y}(u)\right) \Gamma_{\mathrm{E}}^{\mathrm{tf}}\left(\frac{1}{2} \hat{y}(u)\right) \frac{1}{2} g_u(u) \cdot \partial_\xi u\right) \tag{A24}$$

with boundary conditions

$$\left(\widetilde{c}_{\mathrm{E}}^{\mathrm{tot},R}\left(\frac{1}{2} \hat{y}(u)\right) \Gamma_{\mathrm{E}}^{\mathrm{tf}}\left(\frac{1}{2} \hat{y}(u)\right) \frac{1}{2} g_u(u) \cdot \partial_\xi u\right)\Big|_{\xi=0} = \frac{C_h}{\widetilde{D}_{\mathrm{E}}} \tag{A25}$$

$$\left(\widetilde{c}_{\mathrm{E}}^{\mathrm{tot},R}(\frac{1}{2} \hat{y}(u)) \Gamma_{\mathrm{E}}^{\mathrm{tf}}(\frac{1}{2} \hat{y}(u)) \frac{1}{2} g_u(u) \cdot \partial_\xi u\right)\Big|_{\xi=1} = \frac{C_h}{\widetilde{D}_{\mathrm{E}}} \tag{A26}$$

and

$$\widetilde{p} := \widetilde{d} \cdot \widetilde{q}^{\mathrm{V}} \cdot \widetilde{t}_{\mathrm{E}} \tag{A27}$$

The initial value is

$$y_{\mathrm{E}}(x, t = 0) = y_{\mathrm{E}}(\overline{n}_{\mathrm{E}}) \tag{A28}$$

and transfers as

$$u(x, t = 0) = \hat{u}(2y_{\mathrm{E}}(\overline{n}_{\mathrm{E}})). \tag{A29}$$

PDEPE takes the form

$$c(u) \partial_\tau u + \partial_\xi (f(u, \partial_\xi u)) = 0 \tag{A30}$$

with boundary conditions

$$p_l(u|_{x=x_l}) + q_l \cdot f(u, \partial_\xi u)\big|_{x=x_l} = 0 \quad \text{and} \quad p_r(u|_{x=x_r}) + q_r \cdot f(u, \partial_\xi u)|_{x=x_r} = 0. \tag{A31}$$

We have hence

$$c = \widetilde{p} \cdot \frac{C_h}{\widetilde{D}_{\mathrm{E}}} h_{\mathrm{E}}(\frac{1}{2} \hat{y}(u)) \frac{1}{2} g_u(u) \tag{A32}$$

$$f = \widetilde{c}_{\mathrm{E}}^{\mathrm{tot},R}(\frac{1}{2} \hat{y}(u)) \Gamma_{\mathrm{E}}^{\mathrm{tf}}(\frac{1}{2} \hat{y}(u)) \frac{1}{2} g_u(u) \cdot \partial_\xi u \tag{A33}$$

and

$$p_l = \frac{C_h}{\widetilde{D}_{\mathrm{E}}} \qquad p_r = \frac{C_h}{\widetilde{D}_{\mathrm{E}}} \tag{A34}$$

$$q_l = -1 \qquad q_r = -1 \tag{A35}$$

Appendix B: Active Particle

Thermodynamic factor.—We consider for the chemical potential in the active particle phase

$$\mu_{\mathrm{A}} = k_{\mathrm{B}}T\left(\ln\left(\frac{\frac{1}{\omega_{\mathrm{A}}}y_{\mathrm{A}}}{1+\frac{1-\omega_{\mathrm{A}}}{\omega_{\mathrm{A}}}y_{\mathrm{A}}}\right) - \omega\cdot\ln\left(\frac{1-y_{\mathrm{A}}}{1+\frac{1-\omega_{\mathrm{A}}}{\omega_{\mathrm{A}}}y_{\mathrm{A}}}\right) + \gamma_{\mathrm{A}}\cdot h_{\mathrm{A}}(y_{\mathrm{A}})\right) \tag{B1}$$

with

$$g(y) = (2y-1) + \frac{1}{2}\big(6y(1-y)-1\big) - \frac{1}{3}\big(8y(1-y)-1\big)(2y-1) \tag{B2}$$

Hence

$$\frac{\partial\mu_{\mathrm{A}}}{\partial y_{\mathrm{A}}} = \frac{1}{y_{\mathrm{A}}}\frac{1}{(1-y_{\mathrm{A}})(\frac{1}{\omega_{\mathrm{A}}}y_{\mathrm{A}}+(1-y_{\mathrm{A}}))} + \gamma_{\mathrm{A}}\cdot\partial_y g \tag{B3}$$

with

$$\partial_y g = 16\cdot y^2 - 22y_{\mathrm{A}} + \frac{25}{3}. \tag{B4}$$

The thermodynamic factor $\Gamma_{\mathrm{A}}^{\mathrm{tf}}$ is then

$$\Gamma_{\mathrm{A}}^{\mathrm{tf}} = y_{\mathrm{A}}\cdot\frac{\partial f_{\mathrm{A}}}{\partial y_{\mathrm{A}}} = \frac{1}{(1-y_{\mathrm{A}})(\frac{1}{\omega_{\mathrm{A}}}y_{\mathrm{A}}+(1-y_{\mathrm{A}}))} + \gamma_{\mathrm{A}}\cdot(16\cdot y_{\mathrm{A}}^3 - 22y_{\mathrm{A}}^2 + \frac{25}{3}y_{\mathrm{A}}). \tag{B5}$$

PDEPE notation.—We seek to solve 109, i.e.

$$\frac{C_h}{\widetilde{D}_{\mathrm{A}}}\frac{\partial y_{\mathrm{A}}}{\partial\tau} = \partial_\xi\left(y_{\mathrm{A}}\frac{\partial f_{\mathrm{A}}}{\partial y_{\mathrm{A}}}\partial_\xi y_{\mathrm{A}}\right) \tag{B6}$$

with boundary conditions 110

$$y_{\mathrm{A}}\frac{\partial f_{\mathrm{A}}}{\partial y_{\mathrm{A}}}\partial_\xi y_{\mathrm{A}}\big|_{\xi=0} = 0 \quad\text{and}\quad y_{\mathrm{A}}\frac{\partial f_{\mathrm{A}}}{\partial y_{\mathrm{A}}}\partial_\xi y_{\mathrm{A}}\big|_{\xi=1} = \frac{C_h}{\widetilde{D}_{\mathrm{A}}}. \tag{B7}$$

and

$$y_{\mathrm{A}}\frac{\partial f_{\mathrm{A}}}{\partial y_{\mathrm{A}}} = \Gamma_{\mathrm{A}}^{\mathrm{tf}} = y_{\mathrm{A}}\cdot\frac{\partial f_{\mathrm{A}}}{\partial y_{\mathrm{A}}} = \frac{1}{(1-y_{\mathrm{A}})(\frac{1}{\omega_{\mathrm{A}}}y_{\mathrm{A}}+(1-y_{\mathrm{A}}))} + \gamma_{\mathrm{A}}\cdot(16\cdot y_{\mathrm{A}}^3 - 22y_{\mathrm{A}}^2 + \frac{25}{3}y_{\mathrm{A}}). \tag{B8}$$

Note that it is ever convenient for the numerical computation of $y_{\mathrm{A}} \in (0, 1)$ to introduce the variable

$$u = \ln\left(\frac{y_{\mathrm{A}}}{1-y_{\mathrm{A}}}\right) \tag{B9}$$

which yields

$$y_{\mathrm{A}} = \frac{\mathrm{e}^u}{1+\mathrm{e}^u} \tag{B10}$$

We have hence

$$\partial_\tau y_{\mathrm{A}} = \partial_u y_{\mathrm{A}}\cdot\partial_\tau u \tag{B11}$$

and

$$\partial_x y_{\mathrm{A}} = \partial_u y_{\mathrm{A}}\cdot\partial_x u \tag{B12}$$

with

$$\partial_u y_A = \frac{\mathrm{e}^u(1+\mathrm{e}^u) - \mathrm{e}^u\mathrm{e}^u}{(1+\mathrm{e}^u)^2} = \frac{\mathrm{e}^u}{(1+\mathrm{e}^u)^2} =: g(u) \tag{B13}$$

PDEPE takes the form

$$c(u)\partial_\tau u + \partial_\xi(f(u,\partial_\xi u)) = 0 \tag{B14}$$

with boundary conditions

$$p_l(u|_{x=x_l}) + q_l\cdot f(u,\partial_\xi u)\big|_{x=x_l} = 0 \quad\text{and}\quad p_r(u|_{x=x_r}) + q_r\cdot f(u,\partial_\xi u)|_{x=x_r} = 0. \tag{B15}$$

We have hence

$$c = \frac{C_h}{\widetilde{D}_{\mathrm{E}}}g_u(u) \tag{B16}$$

$$f = \Gamma_{\mathrm{A}}^{\mathrm{tf}}(\hat{y}_{\mathrm{A}}(u))g_u(u)\cdot\partial_\xi u \tag{B17}$$

and

$$p_l = 0 \qquad p_r = \frac{C_h}{\widetilde{D}_{\mathrm{E}}} \tag{B18}$$

$$q_l = 1 \qquad q_r = -1 \tag{B19}$$

Note that we introduce the *stop-event* $y_{\mathrm{A}}|_{\mathrm{AE}} < 1 - 10^{-10}$ for the time-integration of pdepe.

List of Symbols

A	Area of the electrode
$C_{\mathrm{E}}^{\mathrm{DL}}$	Double layer capacity
$C_h\,[1]$	C-rate
D_{A}	Active phase diffusion coefficient
$\widetilde{D}_{\mathrm{A}} = \frac{1[\mathrm{h}]}{d_{\mathrm{A}}^2}D_{\mathrm{A}}$	Dimensionless diffusion coefficient in the active phase
D_{E}	Electrolyte diffusion coefficient
E	Measured cell voltage according to 44
$e_0 = 1.602176634\cdot10^{-19}\,[\mathrm{C}]$	Elementary charge
$E_{\mathrm{A,E}}^T$	Intercalation reaction energy
$f_{\mathrm{E}} = \ln\left(\frac{y_{\mathrm{E}_C}}{\left(\hat{y}_{\mathrm{E}_S}(y_{\mathrm{E}_C})\right)^{\kappa_{\mathrm{E}}}}\right)$	Electrolyte reaction potential (see 42)
$g = \mathrm{e}^{\alpha\cdot x} - \mathrm{e}^{-(1-\alpha)\cdot x}$	Reaction rate function
g^{-1}	Inverse reaction rate function
h_{A}	Molar enthalpy function according to 12
i	Current density flowing out of the electrode
$i_{\mathrm{A}}^C = \frac{d_{\mathrm{A}}\cdot q_{\mathrm{A}}^V}{1[\mathrm{h}]}$	1C current density.
$I = A\cdot i$	Measurable current
$I_C = A\frac{d_{\mathrm{A}}\cdot q_{\mathrm{A}}^V}{1[\mathrm{h}]}$	Current with which the battery is charged within one hour
$k_{\mathrm{B}} = 1.380649\cdot10^{-23}\,[\mathrm{JK}^{-1}]$	Boltzmann constant
$\widetilde{L} = \frac{e_0 L_s}{i_{\mathrm{A}}^C}$	Dimensionless exchange current density
L_s	Onsager coefficient of the intercalation reaction
m_α	Molar mass of constituent α in solution
n_α	Molar concentration
$n_{\mathrm{E}}^{\mathrm{tot}} = n_{\mathrm{E}_S} + n_{\mathrm{E}_A} + n_{\mathrm{E}_C}$	Molar concentration of mixing particles in the electrolyte
$n_{\mathrm{E}_S}^R$	Mole density $n_{\mathrm{E}_S}^R$ of the pure solvent
$q_{\mathrm{A}}^{M,\mathrm{NMC}} = 318\,[\mathrm{mA\,h\,g^{-1}}]$	Mass charge density of NMC
$q_{\mathrm{A}}^{V,\mathrm{NMC}} = 1294\,[\frac{\mathrm{mA\,h}}{\mathrm{cm}^3}]$	Volumetric charge density of NMC
$Q = Q_{\mathrm{A}}^V\cdot\bar{y}_{\mathrm{A}_C}$	Electrode capacity
R_s	Surface reaction rate of the intercalation reaction $\mathrm{Li}^+\big\|_{\mathrm{E}} + \mathrm{e}^-\big\|_{\mathrm{A}} \rightleftharpoons \mathrm{Li}\big\|_{\mathrm{A}} + \kappa_{\mathrm{E}}\cdot\mathrm{S}\big\|_{\mathrm{E}}$ according to 38
$S_{\mathrm{E}} = \frac{k_{\mathrm{B}}T}{e_0}\Lambda_{\mathrm{E}}(2t_C - 1)$	Charge diffusion coefficient
t_{E_C}	Cation transfer number
$T = 298.15\,[\mathrm{K}]$	Isothermal temperature
$U_{\mathrm{AE}}^{\mathrm{DL}}$	Potential drop across the double layer of $\Sigma_{\mathrm{A,E}}$
U_i^{SCL}	Space charge layer drop between the surface $\Sigma_{\mathrm{A,E}}$ and the adjacent points $x_{\mathrm{AE}}^{\pm}$ outside the space charge layer
v_α^R	Partial molar volume of constituent α in solution
$V_{\mathrm{A}} = A\cdot d_{\mathrm{A}}$	Volume of the electrode
$x = 0$	Left boundary of Ω_{A} in 1D approximation
$x = x_{\mathrm{AE}}$	Position of $\Sigma_{\mathrm{A,E}}$ in 1D approximation
$x = x_{\mathrm{EC}}$	Right boundary of Ω_{E} in 1D approximation
$y_{\mathrm{A}} = \frac{n_{\mathrm{A}_C}}{n_{\mathrm{A}_\ell}}$	Mole fraction of intercalated cations in the active phase
$\bar{y}_\alpha$	Average mole fraction $\alpha = \mathrm{A}_C, \mathrm{E}_C$

$y_\alpha = \frac{n_\alpha}{n_{\mathrm{E}}^{\mathrm{tot}}}$	Mole fraction (with respect to the number of mixing particles)
z_α	Charge number of constituent α

Greek

κ_{E}	Solvation number of cations and anions in the electrolyte
Ω_{A}	Spatial domain of the active intercalation phase
Ω_{A}	Spatial domain of the electrolyte
$\Sigma_{\mathrm{A,E}}$	Interface between active phase and electrolyte (including electrochemical double layers)
μ_α	Chemical potential (function) for constituent $\alpha = \mathrm{E}_A, \mathrm{E}_C, \mathrm{E}_S, \mathrm{A}_C, \mathrm{A}_e, \mathrm{A}_M$
μ_α	Surface chemical potential (function) for constituent $\alpha = \mathrm{E}_A, \mathrm{E}_C, \mathrm{E}_S, \mathrm{A}_C, \mathrm{A}_e, \mathrm{A}_M$
$\varphi(x, z)$	Electrostatic potential
$\Gamma_{\mathrm{E}}^{\mathrm{tf}}$	Thermodynamic factor electrolyte (see Eq. 25)
Λ_{E}	Molar conductivity
$\Gamma_{\mathrm{E}}^{\mathrm{tf}}$	Thermodynamic factor active phase (see Eq. 36)
σ_{A}	Active phase conductivity
$\lambda_s = e_0(U_{\mathrm{AE}}^{\mathrm{DL}} - E_{\mathrm{A,E}}^T) + k_{\mathrm{B}}T\,(f_{\mathrm{A}} - f_{\mathrm{E}})$	Surface affinity (see Eq. 40)

ORCID

Manuel Landstorfer https://orcid.org/0000-0002-0565-2601

References

1. M. Doyle, T. Fuller, and J. Newman, *J. Electrochem. Soc.*, **140**, 1526 (1993).
2. S.-L. Wu, W. Zhang, X. Song, A. K. Shukla, G. Liu, V. Battaglia, and V. Srinivasan, *J. Electrochem. Soc.*, **159**, A438 (2012).
3. J. Newman, *Transactions of the Faraday Society*, **61**, 2229 (1965).
4. M. Landstorfer, *J. Electrochem. Soc*, **164**, E3671 (2017).
5. W. Dreyer, C. Guhlke, and R. Müller, *Phys. Chem. Chem. Phys.*, **17**, 27176 (2015).
6. I. Müller, *Thermodynamics*, Pitman, 1985.
7. S. de Groot and P. Mazur, *Non-Equilibrium Thermodynamics*, Dover Publications, 1984.
8. W. Dreyer, C. Guhlke, and R. Müller, *Entropy*, **20**, 939 (2018).
9. M. Landstorfer, C. Guhlke, and W. Dreyer, *Electrochim. Acta*, **201**, 187 (2016).
10. W. Dreyer, C. Guhlke, and M. Landstorfer, *Electrochem. Commun.*, **43**, 75 (2014).
11. W. Dreyer, C. Guhlke, and R. Muller, *Phys. Chem. Chem. Phys.*, **15**, 7075 (2013).
12. M. Landstorfer, *Electrochem. Commun.*, **92**, 56 (2018).
13. W. Dreyer, C. Guhlke, M. Landstorfer, and R. Müller, *European J. Appl. Math.*, **29**, 708 (2018).
14. J. W. Cahn and J. E. Hilliard, *J. Chem. Phys.*, **28**, 258 (1958).
15. J. W. Cahn, *J. Chem. Phys.*, **30**, 1121 (1959).
16. R. Garcia, C. Bishop, and W. Carter, *Acta Mater.*, **52**, 11 (2004).
17. W. Dreyer, M. Gaberescek, C. Guhlke, R. Huth, and J. Jamnik, *European J. Appl. Math.*, **22**, 267 (2011).
18. W. Dreyer, C. Guhlke, and R. Huth, *Physica D*, **240**, 1008 (2011).
19. M. Landstorfer, S. Funken, and T. Jacob, *Phys. Chem. Chem. Phys.*, **13**, 12817 (2011).
20. M. Landstorfer and T. Jacob, *Chem. Soc. Rev.*, **42**, 3234 (2013).
21. M. Z. Bazant, *Accounts of Chemical Research*, **46**, 1144 (2013).
22. O. Redlich and A. T. Kister, *Ind. Eng. Chem.*, **40**, 345 (1948).
23. D. K. Karthikeyan, G. Sikha, and R. E. White, *J. Power Sources*, **185**, 1398 (2008).
24. M. Landstorfer, *WIAS Preprint*, 2018.
25. A. Sommerfeld and H. Bethe, in *Aufbau der zusammenhängenden Materie*, Springer, pp. 333, 1933.
26. W. Dreyer, C. Guhlke, and R. Muller, *Phys. Chem. Chem. Phys.*, **18**, 24966 (2016).
27. J. Newman and T. Chapman, *AIChE Journal*, **19**, 343 (1973).
28. J. Newman and K. Thomas, *Electrochemical Systems*, John Wiley & Sons, 2014.
29. R. M. Fuoss, *Journal of Solution Chemistry*, **7**, 771 (1978).
30. R. M. Fuoss and L. Onsager, *The Journal of Physical Chemistry*, **61**, 668 (1957).
31. J. Liu and C. W. Monroe, *Electrochim. Acta*, **135**, 447 (2014).
32. J. Newman, D. Bennion, and C. W. Tobias, *Berichte der Bunsengesellschaft für physikalische Chemie*, **69**, 608 (1965).
33. A. Sanfeld, *Introduction to the thermodynamics of charged and polarized layers*, Wiley, 1968.
34. S. U. Kim and V. Srinivasan, *J. Electrochem. Soc.*, **163**, A2977 (2016).
35. A. Latz and J. Zausch, *J. Power Sources*, **196**, 3296 (2011).
36. A. Sanfeld, A. Passerone, E. Ricci, and J. Joud, *Surface Science Letters*, **219**, L521 (1989).
37. R. Defay, I. Prigogine, and A. Sanfeld, *J. Colloid Interface Sci.*, **58**, 498 (1977).
38. K. A. Jarvis, Z. Deng, L. F. Allard, A. Manthiram, and P. J. Ferreira, *Chemistry of Materials*, **23**, 3614 (2011).
39. K. Shaju and P. Bruce, *Advanced Materials*, **18**, 2330 (2006).
40. A. J. Bard and L. R. Faulkner, *Electrochemical methods: fundamentals and applications*, Wiley New York, vol. 2 1980.
41. T. Fuller, M. Doyle, and J. Newman, *J. Electrochem. Soc.*, **141**, 1 (1994).
42. R. Darling and J. Newman, *J. Electrochem. Soc.*, **144**, 4201 (1997).
43. G. B. Less, J. H. Seo, S. Han, A. M. Sastry, J. Zausch, A. Latz, S. Schmidt, C. Wieser, D. Kehrwald, and S. Fell, *J. Electrochem. Soc.*, **159**, A697 (2012).
44. M. Doyle, J. Newman, A. Gozdz, and C. Schmutz, *J. Electrochem. Soc.*, **143**, 1890 (1996).
45. Q. Zhang, Q. Guo, and R. White, *J. Electrochem. Soc.*, **153**, A301 (2006).
46. A. Latz, J. Zausch, and O. Iliev, in *Numerical Methods and Applications*, ed. I. Dimov, S. Dimova, and N. Kolkovska, Springer Berlin/Heidelberg, vol. 6046 of Lecture Notes in Computer Science, pp. 329, 2011.
47. W. Lai and F. Ciucci, *Electrochim. Acta*, **56**, 4369 (2011).
48. A. Jokar, B. Rajabloo, M. Désilets, and M. Lacroix, *J. Power Sources*, **327**, 44 (2016).
49. R. Spotnitz, *Battery Design Studio* (http://www.batdesign.com/).
50. P.-C. Tsai, B. Wen, M. Wolfman, M.-J. Choe, M. S. Pan, L. Su, K. Thornton, J. Cabana, and Y.-M. Chiang, *Energy Environ. Sci.*, **11**, 860 (2018).
51. A. Latz and J. Zausch, *Electrochim. Acta*, **110**, 358 (2013).
52. N. Nitta, F. Wu, J. T. Lee, and G. Yushin, *Materials Today*, **18**, 252 (2015).